PB85-138279

Hazardous Air Pollutants Dry-Deposition Phenomena

Battelle Pacific Northwest Labs., Richland, WA

Prepared for

Environmental Sciences Research Lab.
Research Triangle Park, NC

Dec 84

U.S. Department of Commerce
National Technical Information Service
NTIS

PB85-138279

EPA-600/3-84-114
December 1984

HAZARDOUS AIR POLLUTANTS: DRY-DEPOSITION PHENOMENA

by

G.A. Sehmel, R. N. Lee, T. W. Horst

Pacific Northwest Laboratory
Richland, WA 99352

IAG DW930193

Project Officer

Larry T. Cupitt
Atmospheric Chemistry and Physics Division
Atmospheric Sciences Research Laboratory
Research Triangle Park, NC 27711

ATMOSPHERIC SCIENCES RESEARCH LABORATORY
OFFICE OF RESEARCH AND DEVELOPMENT
U.S. ENVIRONMENTAL PROTECTION AGENCY
RESEARCH TRIANGLE PARK, NC 27711

REPRODUCED BY
NATIONAL TECHNICAL
INFORMATION SERVICE
U.S. DEPARTMENT OF COMMERCE
SPRINGFIELD, VA. 22161

TECHNICAL REPORT DATA
(Please read Instructions on the reverse before completing)

1. REPORT NO.	2.	3. RECIPIENT'S ACCESSION NO.
EPA-600/3-84-114		PB85 138279

4. TITLE AND SUBTITLE	5. REPORT DATE
HAZARDOUS AIR POLLUTANTS: DRY-DEPOSITION PHENOMENA	December 1984
	6. PERFORMING ORGANIZATION CODE
7. AUTHOR(S)	8. PERFORMING ORGANIZATION REPORT NO.
G. A. Sehmel, R. N. Lee, and T. W. Horst	
9. PERFORMING ORGANIZATION NAME AND ADDRESS	10. PROGRAM ELEMENT NO.
Pacific Northwest Laboratory Richland, WA 99352	C9TA1B/01-2022 (FY-85)
	11. CONTRACT/GRANT NO.
	IAG DW930193
12. SPONSORING AGENCY NAME AND ADDRESS	13. TYPE OF REPORT AND PERIOD COVERED
Atmospheric Sciences Research Laboratory, RTP, NC Office of Research and Development U.S. Environmental Protection Agency Research Triangle Park, North Carolina 27711	14. SPONSORING AGENCY CODE EPA/600/09

15. SUPPLEMENTARY NOTES

16. ABSTRACT

Dry-deposition rates were evaluated for two hazardous organic air pollutants, nitrobenzene and perchloroethylene, to determine their potential for removal from the atmosphere to three building material surfaces, cement, tar paper, and vinyl asbestos tile. Dry-deposition experiments were conducted in two stirred chambers. Building materials were placed on the bottom of the stirred chambers, and removal rates were evaluated by introducing the organic air pollutant along with nondepositing sulfur hexafluoride (SF_6) tracer gas into a stirred chamber. Changes in airborne concentrations with time were then monitored. Because the HAP removal rates were small, sulfur hexafluoride tracer gas was used to evaluate the rates of leakage from the SC in order to correct the deposition rates. When HAP wall losses were assumed negligible, HAP concentration decreases (corrected using the SF_6 leakage rate) ranged from near 0 to 3 %/h. Dry-deposition velocities were calculated from the rate-of-change over time of the airborne concentrations. The calculated deposition velocities were consistently small, approximately 10^{-4} cm/sec or less. These deposition velocities reflect mostly substrate resistance, but the fan speed could not be increased sufficiently to ensure in the limit that only substrate resistance was measured.

17. KEY WORDS AND DOCUMENT ANALYSIS

a. DESCRIPTORS	b. IDENTIFIERS/OPEN ENDED TERMS	c. COSATI Field/Group

18. DISTRIBUTION STATEMENT	19. SECURITY CLASS *(This Report)*	21. NO. OF PAGES
RELEASE TO PUBLIC	UNCLASSIFIED	80
	20. SECURITY CLASS *(This page)*	22. PRICE
	UNCLASSIFIED	

EPA Form 2220-1 (Rev. 4-77) PREVIOUS EDITION IS OBSOLETE

NOTICE

The information in this document has been funded wholly by the United States Environmental Protection Agency under IAG DW930193 to Pacific Northwest Laboratory. It has been subject to the Agency's peer and administrative review, and it has been approved for publication as an EPA document. Mention of trade names or commercial products does not constitute endorsement or recommendation for use.

ABSTRACT

Dry-deposition rates were evaluated for two hazardous organic air pollutants (HAPs) to determine their potential for removal from the atmosphere to three building material surfaces. The organic air pollutants were nitrobenzene and perchloroethylene; the building materials used were cement, tar paper, and vinyl asbestos tile. Dry-deposition experiments were conducted in two stirred chambers (SC) that were originally designed and constructed to permit determination of removal rates to vegetation in the environment. Throughout this research, the chambers were located indoors. Building materials were placed on the bottom of the stirred chambers, and removal rates were evaluated by introducing the organic air pollutant along with nondepositing sulfur hexafluoride (SF_6) tracer gas into a stirred chamber. Changes in airborne concentrations with time were then monitored.

Because the HAP removal rates were small, sulfur hexafluoride tracer gas was used to evaluate the rates of leakage from the SC in order to correct the deposition rates. When HAP wall losses were assumed to be negligible, HAP concentration decreases (corrected using the SF_6 leakage rate) ranged from near 0 to 3% h^{-1}. Dry-deposition velocities were calculated from the rate-of-change over time of the airborne concentrations. The calculated deposition velocities were consistently small, approximately 10^{-4} cm s^{-1} or less. These deposition velocities reflect mostly substrate resistance, but the fan speed could not be increased further to ensure, in the limit, that only substrate resistance was measured.

CONTENTS

ABSTRACT iii

FIGURES vi

TABLES viii

1. Introduction 1

2. Conclusions and Recommendations 3

3. Measurement Methodology 5

4. Data Collection 14

5. Data Interpretation and Generalization 20

6. Deposition Modeling Development 23

References 29

Appendices

A. Analytical Techniques 31

B. Tests of Stirred Chamber Leakage and Wall Loss 35

C. HAP and SF_6 Concentration Loss Rates 41

D. HAP and SF_6 Concentration Data 58

FIGURES

Number		Page
1	Schematic of a stirred chamber	8
2	Schematic elevation and plan views of model layout	25
B-1	SF_6 Concentration decrease with time in empty stirred chambers	36
B-2	Run 5-1: Perchloroethylene and SF_6 tracer gas concentration decreases for empty SC number 1	37
B-3	Run 5-2: Perchloroethylene and SF_6 tracer gas concentration decreases for empty SC number 2	38
C-1	Run 1-1: Perchloroethylene and SF_6 tracer gas concentration decreases for 10.0 m^2 of cement block deposition surface	41
C-2	Run 1-2: Perchloroethylene and SF_6 tracer gas concentration decreases for 6.1 m^2 of cement block deposition surface	42
C-3	Run 2-1: Perchloroethylene and SF_6 tracer gas concentration decreases for 10.0 m^2 of cement block deposition surface	43
C-4	Run 2-2: Perchloroethylene and SF_6 tracer gas concentration decreases for 6.1 m^2 of cement block deposition surface	44
C-5	Run 4-1: Perchloroethylene and SF_6 tracer gas concentration decreases for 10.0 m^2 of cement block deposition surface	45
C-6	Run 4-2: Perchloroethylene and SF_6 tracer gas concentration decreases for 6.1 m^2 of cement block deposition surface	46
C-7	Run 6-1: Perchloroethylene and SF_6 tracer gas concentration decreases for 6.0 m^2 of vinyl asbestos tile deposition surface	47
C-8	Run 7-1: Perchloroethylene and SF_6 tracer gas concentration decreases for 6.0 m^2 of tar paper deposition surface	48

FIGURES (CONTD)

Number		Page
C-9	Run 8-2: Perchloroethylene and SF_6 tracer gas concentration decreases for 6.0 m^2 of vinyl asbestos tile deposition surface	49
C-10	Run 9-1: Perchloroethylene and SF_6 tracer gas concentration decreases for 6.0 m^2 of tar paper deposition surface	50
C-11	Run 10-2: Perchloroethylene and SF_6 tracer gas concentration decreases for 6.0 m^2 of vinyl asbestos tile deposition surface	51
C-12	Run 11-1: Perchloroethylene and SF_6 tracer gas concentration decreases for 6.0 m^2 of tar paper deposition surface	52
C-13	Run 15-1: Nitrobenzene and SF_6 tracer gas concentration decreases for 6.0 m^2 of tar paper deposition surface	53
C-14	Run 16-2: Nitrobenzene and SF_6 tracer gas concentration decreases for 6.0 m^2 of vinyl asbestos tile deposition surface	54
C-15	Run 17-1: Nitrobenzene and SF_6 tracer gas concentration decreases for 6.0 m^2 of tar paper deposition surface	55
C-16	Run 18-2: Nitrobenzene and SF_6 tracer gas concentration decreases for 6.0 m^2 of vinyl asbestos tile deposition surface	56
C-17	Run 19-1: Nitrobenzene and SF_6 tracer gas concentration decreases for 6.0 m^2 of tar paper deposition surface	57

TABLES

Number		Page
1	Primary compounds of interest	1
2	Dry deposition velocity ranges for gas	6
3	Predicted HAP loss rates in a stirred chamber	13
4	HAP detection limits	15
5	Summary of stirred chamber losses	18
6	HAP dry-deposition velocities	19
B-1	Run 5-1: Perchloroethylene and SF_6 tracer gas concentration decreases for an empty SC	39
B-2	Run 5-2: Perchloroethylene and SF_6 tracer gas concentration decreases for an empty SC	39
B-3	Empty stirred chamber losses	40
D-1	Run 1-1: Perchloroethylene and SF_6 tracer gas concentration decreases for 10.0 m^2 of cement block deposition surface	59
D-2	Run 1-2: Perchloroethylene and SF_6 tracer gas concentration decreases for 6.1 m^2 of cement block deposition surface	60
D-3	Run 2-1: Perchloroethylene and SF_6 tracer gas concentration decreases for 10.0 m^2 of cement block deposition surface	61
D-4	Run 2-2: Perchloroethylene and SF_6 tracer gas concentration decreases for 6.1 m^2 of cement block deposition surface	62
D-5	Run 4-1: Perchloroethylene and SF_6 tracer gas concentration decreases for 10.0 m^2 of cement block deposition surface	63
D-6	Run 4-2: Perchloroethylene and SF_6 tracer gas concentration decreases for 6.1 m^2 of cement block deposition surface	63

TABLES (CONTD)

Number		Page
D-7	Run 6-1: Perchloroethylene and SF_6 tracer gas concentration decreases for 6.0 m^2 of vinyl asbestos tile deposition surface	64
D-8	Run 7-1: Perchloroethylene and SF_6 tracer gas concentration decreases for 6.0 m^2 of tar paper deposition surface	65
D-9	Run 8-2: Perchloroethylene and SF_6 tracer gas concentration decreases for 6.0 m^2 of vinyl asbestos tile deposition surface	66
D-10	Run 9-1: Perchloroethylene and SF_6 tracer gas concentration decreases for 6.0 m^2 of tar paper deposition surface	66
D-11	Run 10-2: Perchloroethylene and SF_6 tracer gas concentration decreases for 6.0 m^2 of vinyl asbestos tile deposition surface	67
D-12	Run 11-1: Perchloroethylene and SF_6 tracer gas concentration decreases for 6.0 m^2 of tar paper deposition surface	67
D-13	Run 15-1: Nitrobenzene and SF_6 tracer gas concentration decreases for 6.0 m^2 of tar paper deposition surface	68
D-14	Run 16-2: Nitrobenzene and SF_6 tracer gas concentration decreases for 6.0 m^2 of vinyl asbestos tile deposition surface	68
D-15	Run 17-1: Nitrobenzene and SF_6 tracer gas concentration decreases for 6.0 m^2 of tar paper deposition surface	69
D-16	Run 18-2: Nitrobenzene and SF_6 tracer gas concentration decreases for 6.0 m^2 of vinyl asbestos tile deposition surface	69
D-17	Run 19-1: Nitrobenzene and SF_6 tracer gas concentration decreases for 6.0 m^2 of tar paper deposition surface	70

SECTION 1

INTRODUCTION

The research project, Hazardous Air Pollutants: Dry-Deposition Phenomena, is being conducted to provide information that will advance the U.S. Environmental Protection Agency's (EPA) capability to understand the rates and mechanisms of dry-deposition removal of certain critical organic compounds (see Table 1). Through this project, the dry-deposition removal rates will be incorporated into a general predictive atmospheric transport, diffusion, and deposition model. The MPADD (Multi-Pollutant Atmospheric Deposition and Depletion) model, was developed concurrently in this project and in a companion project for the EPA on Hazardous Air Pollutants: Wet Removal Rates and Mechanisms (1).

TABLE 1. PRIMARY COMPOUNDS OF INTEREST

Carbon tetrachloride	CCl_4
Chloroform	$CHCl_3$
Ethlyene dichloride	$H_2ClCCClH_2$
Methylchloroform	Cl_3CCH_3
Methylene chloride	CH_2Cl_2
Nitrobenzene	$C_6H_5NO_2$
Perchloroethylene	Cl_2CCCl_2
Phosgene	$COCl_2$
Polychlorinated biphenyls, (PCB's)	(C_6H_6) chlorine adducts
1,1,2-trichloro-1,2,2-trifluoro-ethane, (Freon 113)	Cl_2FCCF_2C

To determine dry-deposition removal rates of organic hazardous air pollutants (HAPs), we must design and use an adequate and reliable method. We also must select the appropriate pollutant compounds and deposition substrates (some representative primary compounds of interest and some substrates typical of urban areas). The project is divided into four major components, each of which is necessary to fulfill these goals.

1. design and construction of stirred chambers
2. collection of data from stirred chambers
3. interpretation of data
4. deposition modeling.

All dry-deposition measurements were made in stirred chambers (SCs) located in a room. The SC is an inert-surface box within which are placed selected deposition surfaces. The principal advantage of using the SC is that concentrations can be controlled within manageable limits throughout the duration of each experiment. During the experiments, the SCs were sealed to minimize leakage and charged with a preselected atmosphere of HAP and SF_6 tracer gas that was mixed continuously using an open fan. Concentrations within the SC were monitored intermittently for specified time periods depending on the concentration decay rate. Deposition rates were then calculated on the basis of concentration-decay rates.

Seventeen experiments were conducted to determine the maximum removal rates for HAP's to large deposition-surface areas. Dry-deposition velocities of perchloroethylene were evaluated during twelve experiments with cement, tile, and tar paper substrates. Deposition velocities of nitrobenzene were evaluated during five experiments with tile and tar paper substrates. The velocities were calculated from airborne concentration losses of HAP and SF_6 tracer gas with time. The nondepositing SF_6 tracer gas was used to measure HAP leakage rates from the stirred chambers. These measurements of HAP dry-deposition velocities can be used in the general predictive atmospheric transport, diffusion, and deposition model MPADD (Multi-Pollutant Atmospheric Deposition and Depletion).

Conclusions of the study and recommendations for further research are given in Section 2 of this report. The following four sections detail progress on each of the four components listed above. All relevant experimental data are presented in the Appendices.

SECTION 2

CONCLUSIONS AND RECOMMENDATIONS

The removal of gaseous organic air pollution by dry deposition has not been studied extensively and few experimental data are available. Hence, obtaining dry-deposition velocities for nitrobenzene and perchloroethylene is a significant advance in the understanding of organic removal rates. Measured deposition velocities were significantly less than those usually reported for inorganic gases. Deposition velocities were consistently low: many were not significantly different from zero.

Temperature effects were not intensively investigated since all successful experiments were conducted in warm summer weather (ambient temperatures from 27 to 36°C). Because the dry-deposition velocities measured for the two HAPs investigated were low, we can conclude that airborne concentrations of HAP are not significantly reduced by dry deposition at temperatures characteristic of summer months, or at temperatures maintained within buildings. Vapor pressure, however, is anticipated to be a very important property influencing dry-deposition removal rates for organic gases.

The SC approach for evaluating HAP dry-deposition velocities was adequate for the HAPs and substrates investigated. Leakage was always observed, and leakage rates tended to increase during the experimental series. To alleviate this problem, the SCs were periodically maintained by replacing critical seals or tightening the bolts holding sections of the chambers together to minimize exchange with outside air.

One important advantage of the SC technique is that a large substrate surface area can be contained for the deposition substrate. Even though dry-deposition velocities might be low, they could be a function of spatial variations in substrate characteristics. Hence, by using the relative large surface area in an SC (6.0-m^2 floor area), average dry-deposition velocities can be evaluated over these spatial variations.

We recommend that the SC approach be used to evaluate additional HAP and deposition substrates. However, other measurements techniques should be considered. Thermogravimetric techniques may be useful as a screening method to evaluate maximum removal rates for small surface areas on the order of 1 cm^2. This technique may be essential for evaluating deposition velocities less than about 10^{-6} cm/s. Flow-through chambers may be considered if the removal rates are significantly greater than those evaluated in the current experiments. Instrumentation with high sensitivity and rapid analysis techniques would be required if flow-through chambers were used.

We also recommend that dry-deposition velocities be evaluated for additional construction materials, and for vegetative canopies and water surfaces. Currently, no data exist for predicting HAP dry-deposition velocities for vegetation and soils. Possible sorbtion by surface moisture is important. Dry-deposition velocities of HAPs onto these dry construction materials appear lower than dry deposition velocities for other gases that were evaluated for vegetative canopies.

SECTION 3

MEASUREMENT METHODOLOGY

The description of measurement methodology is divided into discussions of SC rationale, substrate selection, HAP selection, SC design, and calculation of deposition velocity from SC measurements. For experimental design purposes, the methodology was based on the assumption that HAP dry-deposition velocities would be comparable to those for other gases. The ranges of deposition velocities shown in Table 2 were considered in establishing the SC rationale. Reported dry-deposition velocities for fifteen gases were summarized by Sehmel (2) in 1980, and for CH_3I and CCl_4 by Cupitt (3) in 1980.

Table 2 shows that except for the noble gas krypton, which is unreactive (hence a very low deposition velocity), and CCl_4, dry-deposition velocities for gases are greater than 10^{-4} cm/s. With the exception of $(CH_3)_2S$, deposition velocities for all other gases are greater than 10^{-3} cm/s.

SC RATIONALE

Originally, our research was directed toward evaluating maximum dry-deposition velocities for reasonably large surfaces. This included vegetation canopies growing in the environment. Hence, the main reason for selecting the portable SC experimental approach was that it approximated field conditions. In principle, this experimental approach allowed us to evaluate deposition substrate areas as large as 6 m^2 and vegetative canopy heights up to 1.5 m.

Before the SC design was completed. questions relating to both structural features and materials were addressed in detail. Proposed substrates included flat surfaces such as ground and pavement, and readily available vegetative canopies such as grass, alfalfa, and sagebrush. A literature review (4) revealed that in past studies, outdoor photochemical chambers were used to investigate the behavior of airborne pollutants under 'natural' conditions.

TABLE 2. DRY-DEPOSITION VELOCITY RANGES FOR GASES

Depositing gas	Deposition velocity range (cm/s)
SO_2	0.04 to 7.5
I_2	0.02 to 26
HF	1.6 to 3.7
ThB	0.08 to 2.6
Fluorides	0.03 to 2.4
Cl_2	1.8 to 2.1
O_3	0.002 to 2.0
NO_2	1.9
NO	minus to 0.9
PAN	0.8
NO_x	minus to 0.5
H_2S	0.015 to 0.38
CO_2	0.3
$(CH_3)_2S$	10-4 to 10-2
Kr	2.3×10^{-11}
CH_3I	10^{-4} to 10^{-2}
CCl_4	10^{-4}

We considered the chambers used in these studies to incorporate design features that provided the physical strength required to withstand wind and other environmental stresses. After searching the literature and making some preliminary tests, we decided that

- the SC geometry should minimize spaces with low air circulation
- wall surfaces should be Teflon® sheeting to reduce wall losses
- the sheeting joints should be sealed with U-channels attached to the supporting framework.

® Registered trademark of the DuPont Company, Wilmington, Deleware.

SC DESIGN

Because the original intention of these studies included evaluating dry-deposition velocities to vegetative deposition substrates under natural outdoor conditions, the SC walls were constructed of Teflon, which allowed light transmission to ensure vegetation growth while being inert to deposition. The SC was configured to allow us to determine dry-deposition removal rates on both horizontal and vertical surfaces.

Two identical SC units were fabricated to allow us to conduct experiments in parallel and compare pollutant behavior. Parallel experiments made efficient use of chamber operator and analysis time. Each SC was assembled from subassemblies consisting of three sides of hexagonal geometry. In addition, segments of the two identical SC units could be assembled together to evaluate deposition to taller vegetative canopies in one SC. For experiments involving vegetation, the SC height can be increased to 1.5 m, by constructing one SC from four hexagonal subassemblies that are attached together. Two subassemblies are used to form the SC from ground level to 0.8 m, and the remaining two subassemblies are used to form the SC from a height of 0.8 to 1.5 m.

An SC is shown schematically in Figure 1. The supporting structure was constructed with wooden 2 x 4's and plywood. The walls, ceiling, and floor are 5-mil Teflon sheeting. The SC is hexagonal with an internal height of 74 cm and six internal sides of 152 cm. The maximum internal horizontal dimension is 304 cm, the internal volume is 4.4 m^3, and the floor area is 6.0 m^2.

Important features in Figure 1 are the stirring fan, sampling septa, and the charcoal purge system. The fan at the top of the SC has a variable speed motor for investigating HAP removal rates as a function of increasing turbulence and wind speed. The SC design allows us to evaluate removal rates at increasing fan speeds until removal rates become independent of increasing fan speed. The fan is three bladed, with 18 in.-diameter blades and a 25° pitch, coated with Teflon, and powered by a 1/8 hp-motor. Three sets of sampling septa are located along chamber radii spaced at 120°. In each

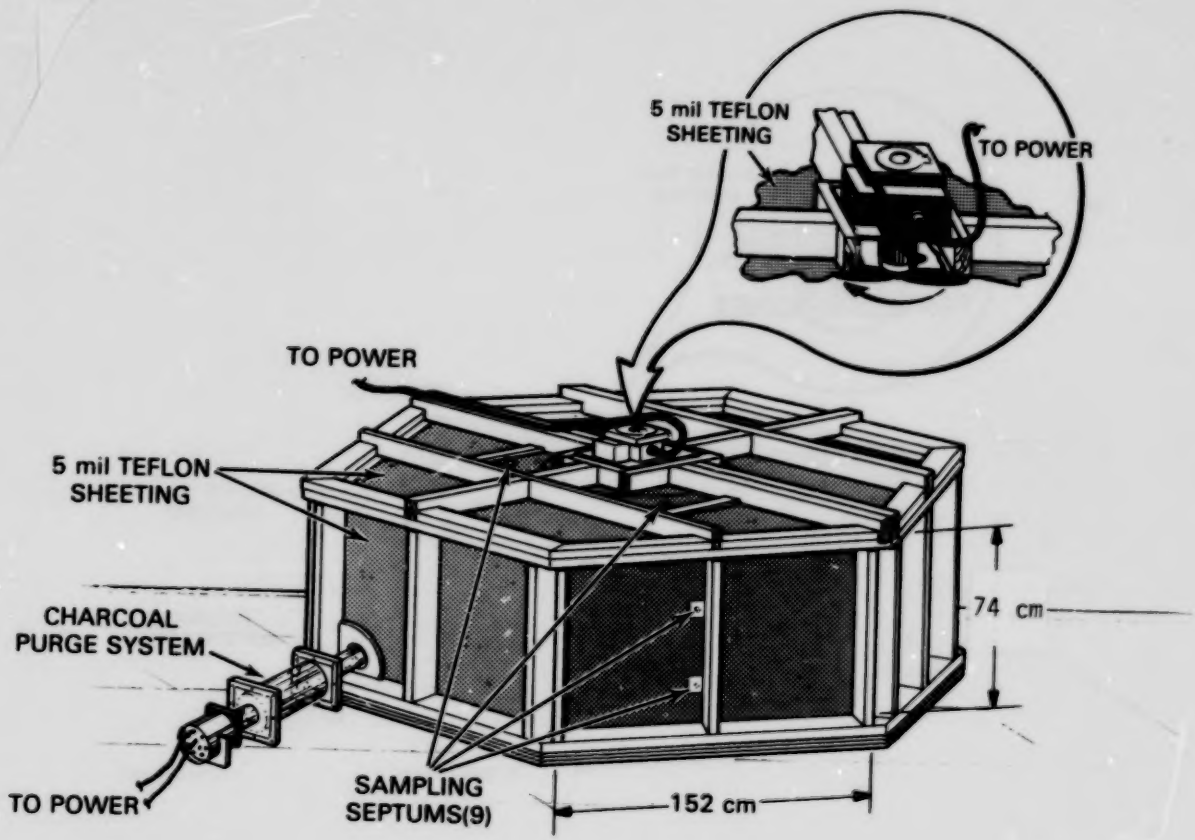

Figure 1. Schematic of a stirred chamber.

set, two septa are located along the chamber side wall and one septum along the chamber ceiling.

The charcoal purge system was designed to remove residual HAP from the SC after each experiment. A similar system without an air pump is located on the opposite wall of the SC. This is an air inlet system for introducing clean air into the SC.

In order to seal the SC, Teflon sheeting was stapled to the wooden frame work. Subsequently, Teflon encased U-channels were screwed over the staples. By screwing the U-channels down tightly, the open side of the U-channel was pressed against the Teflon sheeting and made an effective seal.

SUBSTRATE SELECTION

Originally, deposition substrates were chosen to represent an extended range of materials of practical interest. These were divided into living and nonliving substrates. Nonliving substrates include asphalt, fresh water, and simulated seawater. Living substrates were grouped into three types, that were chosen to maximize coverage of practical vegetation classes.

After construction of the SCs had begun, EPA indicated that they were currently more interested in deposition to typical urban surfaces than to living substrates. Therefore, we selected deposition substrates that represented typical construction materials: cement, tar paper, and vinyl asbestos tile. Cement was selected because it is used for floors and walls in industry and home construction, and for streets and highways. The cement was patio block [20 x 40 x 4.1 cm (7-3/4 x 15-3/4 X 1-5/8 in.)] configured on the floor of the SCs. Two cement block configurations were used to change the available surface area for deposition, either 6.1 or 10 m^2. Similarly, vinyl asbestos tile was selected because it is a floor covering used in industry and homes. Tar paper was selected because it has a high organic content, which might affect HAP removal rates. Both the vinyl asbestos tile and the tar paper were placed to uniformly cover the SC floor.

HAP SELECTION

The HAP gases studied were chosen to encompass a range of chemical and physical properties. Additional considerations such as analytical sensitivity, toxicity, availability from the vendor, and the ease of handling and analyzing were also important to the decision process. These factors played a major role in defining the order in which the materials selected from Table 1 should be addressed.

Perchloroethylene was chosen for the initial experiments because chlorocarbons dominate the list of compounds of interest and it has low toxicity and is easy to analyze. Nitrobenzene was selected for subsequent experiments after evaluating the analytical protocols. An additional reason for using perchloroethylene and nitrobenzene was that analytical development costs were reduced. We already had experience in the analytical procedures for these two gases and a sufficient supply of both materials were available to complete the SC studies (1).

Using both perchloroethylene and nitrobenzene allowed us to investigate varying physical and chemical properties. The gases differ significantly in their boiling points and hence vapor pressures. The boiling point for perchloroethylene is 121.2°C and for nitrobenzene is 210.9°C.

CALCULATION OF DRY-DEPOSITION VELOCITY FROM SC MEASUREMENTS

Deposition velocities were evaluated by introducing both HAP and nondepositing SF_6 tracer gas into an SC located in a room, mixing the gas with the fan, and sampling airborne concentrations as a function of time. The plan was to evaluate the maximum HAP removal rate during several experiments by increasing the fan speed until the removal rate was independent of fan speed (i.e., surface mass transfer resistance was to be decreased by the increased air motion).

The dry-deposition velocities were calculated from the measured rates of decrease in the SF_6 and HAP concentrations. Because the SF_6 tracer

is nondepositing, the HAP volumetric leak rate from the SC is assumed equal to the SF_6 volumetric leak rate. In general, both HAP and SF_6 concentration decreases are described by

$$V \frac{dC}{dt} = -L\ C \qquad (1)$$

where C = airborne concentration
V = chamber volume (4.4 m^3)
L = volumetric leak rate
t = time.

After integrating from C_o at t = 0, Equation 1 reduces to

$$\ln \frac{C}{C_o} = -\frac{L}{V}\ t \qquad (2)$$

Because rates of concentration decrease are actually measured, Equation 2 is rearranged to describe the loss rates for both HAP and SF_6:

$$\frac{L}{V} = -\ (\ln \frac{C}{C_o})\ (\frac{1}{t}) \qquad (3)$$

Velocities are calculated from the time rate-of-change of test gas concentrations in the SC. Assuming that stirring produces uniform gas concentrations within the chamber, a mass balance gives

$$V \frac{dC}{dt} = -v_{ds}\ C\ A_s - v_{dw}\ C\ A_w - CL \qquad (4)$$

where V = volume of the test chamber
A_s = area of the test substrate
A_w = area of the chamber walls
v_{ds} = deposition velocity of the test gas to the substrate of interest
v_{dw} = deposition velocity to the wall surfaces.

After Equation 4 is integrated and rearranged, the concentration decreases for both HAP and SF_6 (Equation 3) are introduced and the dry-deposition velocity is calculated from the expression

$$v_{ds} = (1/A_s) \left\{ V\left[(L/V)_{HAP} - (L/V)_{SF_6}\right] - v_{dw} A_w \right\} \qquad (5)$$

The deposition velocity is in units of cm/s when area is in units of cm^2, volume is in units of cm^3, and normalized leakage rates, (L/V), are in units of fraction loss per second. Thus, in using Equation 5, the deposition velocity to the substrate in the SC is evaluated directly from knowledge of the chamber geometry and the time rate-of-change of gas concentrations.

To show that the SC technique was applicable (i.e., measurements of HAP loss rates would be accurate enough to determine deposition velocities), we calculated HAP loss rates for assumed dry-deposition velocities. In these calculations, wall losses (v_{dw}) and volumetric leak rates (L) were assumed negligible, and deposition was assumed for a substrate uniformly covering the entire 6.0 m^2 of the SC floor. In this case, Equation 5 reduces to

$$v_{ds} = (V/A_s) \quad (L/V)_{HAP} \qquad (6)$$

Because loss rates are subsequently reported in percent loss per hour, Equation 6 further reduces to

$$v_{ds} = [(4.4 \times 10^6)/(6.0 \times 10^4)] \times [(\text{percent loss/h})/(100 \times 3600)]$$

$$= (2.0 \times 10^{-4}) \text{ (percent loss/h)} \qquad (7)$$

Predicted HAP loss rates are shown in Table 3 for a range of dry deposition velocities typical of gases (see Table 2).

TABLE 3. PREDICTED HAP LOSS RATES IN A STIRRED CHAMBER

Assumed dry-deposition velocity cm/s)	Predicted HAP concentration loss rate (%/h)
2×10^{-3}	10
10^{-3}	5
2×10^{-4}	1
10^{-4}	0.5

Loss rates of HAP in the SC were predicted to range from 0.5 to 10 %/h. Thus, HAP loss rates were expected to be measureable for the expected range of dry-deposition velocities.

SECTION 4

DATA COLLECTION

The ultimate objective of these SC investigations was to provide an essentially multidimensional coverage of key variables affecting HAP deposition. This was initially visualized as a four-dimensional matrix of properties:

- Dimension 1 -- chemical composition
- Dimension 2 -- substrate type
- Dimension 3 -- concentration
- Dimension 4 -- substrate variables (growth stage, diurnal status, horizontal surface, vertical surface, etc.).

Dry-deposition velocities should be a function of variables in each dimension. For instance, HAP chemical and physical properties can affect mass transfer rates at the surface of the deposition substrate. If the HAP is very reactive chemically or of low vapor pressure, removal rates are expected to increase. Chemical reactivity also is a function of substrate characteristics and the amount of surface deactivation caused by prior deposition. In our experiments, however, only chemical composition and substrate type were investigated, because a large amount of time was required to construct and 'debug' the chambers and to reduce leakage problems.

The initial pollutant concentrations in the SC were established to be as low as practical, but still sufficiently high to permit rapid quantitative analysis without preconcentrating the samples withdrawn from the SC for chemical analysis. Approximate gas chromatographic detection limits are shown in Table 4 for the two pollutants investigated; actual initial test concentrations of perchloroethylene in the SCs (see Appendix D) were roughly two orders of magnitude higher than detection limits.

TABLE 4. HAP DETECTION LIMITS

Gas	Detection limits [ppb (v/v)]
Nitrobenzene	~1200
Perchloroethylene	0.4

SC CHARGING AND SAMPLING PROCEDURES

The SCs were charged with the species of interest and SF_6 tracer gas by syringe injection. The SF_6 was added as pure gas using a gas-tight 25-µl syringe. In contrast, perchloroethylene and nitrobenzene were added by withdrawing head space vapors from a bottle containing the pure compound. The 30-µl syringe used for transfer to the SCs was used solely for this purpose and stored in a fume hood isolated from the SC and analytical laboratory during chamber experiments.

Standard whole-air sampling procedures were followed for the analysis of volatile materials, but because nitrobenzene has a much higher detection limit, those samples required preconcentration from a large sample volume. The analytical protocols used are described in Appendix A. The frequency of sample withdrawal and analysis were dependent on the observed depletion rate. In general, samples were taken hourly. Integrated samples (nitrobenzene) were collected over periods of several minutes and the sampling time reported as the midpoint in the sample collection period.

SF_6 LEAKAGE RATES

Decreases in concentration that result from leakage must be determined to evaluate HAP removal rates to the substrates of interest. Therefore, preliminary tests using an inert tracer gas, SF_6, were conducted to evaluate the experimental design and control measures. Leakage was monitored both in the chamber and along the periphery of the SC. Excessive leakage locations were sealed when identified.

Sulfur hexafluoride concentration decreases with time are shown in Appendix B (Figure B-1) for the two chambers, numbered 1 and 2. Concentrations were normalized to the initial sampled concentrations of SF_6 tracer gas, C_o, in each chamber. In the example shown, concentration decreases were monitored for 46 h.

The L/V loss rate was about 1 %/h for SF_6 tracer gas (nondepositing). In chamber 1 the loss rate decreased at the 43 and 46 h sampling times. Possibly, this decrease in loss rate for chamber 1 reflects some aging effects.

HAP REMOVAL RATES

After preliminary tests with SF_6 were completed, tests were begun using both gases (i.e., HAP and SF_6) with the chambers in a room. At time zero, the chamber was charged with a preselected concentration of HAP and inert tracer gas; then concentrations within the chamber were monitored to provide a time series of HAP and tracer gas decay within the chamber. In some cases, both SCs were used to conduct parallel runs to assess the reproducibility of the experiment.

Stirred chamber experiments were conducted with either perchloroethylene (and SF_6), or nitrobenzene (and SF_6). Normalized concentration decays with time for both HAP and SF_6 in each experiment are shown in Appendix C (Figures C-1 through C-17), and numerical values for concentrations and times are listed in Appendix D. Concentrations at time zero, C_o, are listed in Appendix D. After time zero, concentrations tended to decrease exponentially with time. Hence for graphical representation, measured concentrations were divided by C_o. Least-squares lines and losses (percent per hour) are shown in each figure. Results are summarized in Table 5.

Both HAP and SF_6 loss rates were significant and ranged from 1.44 to 7.19% lost per hour. When wall losses were assumed negligible (see Appendix B) and leakage rates were corrected, the HAP deposition losses ranged from near zero to about 3% lost per hour.

Possibly because of the limited range of substrate area and fan speed investigated, we found that neither substrate area (either 6.1 or 10.0 m^2 for cement) nor increased fan speed (experiments 4, 10, and 11) significantly affected HAP loss rates. Only two fan speeds were used: 520 rpm and a motor-limited maximum rpm of 600. Nearly all experiments were conducted at a fan speed of 520 rpm.

Although losses tended to be exponential with time, other time-dependent effects were apparent. Concentrations increased immediately after gas injection and continued to increase until a maximum concentration was observed. Subsequently, concentrations tended to be exponential with time as described by the equations from which dry-deposition velocities are calculated. Also, deviations from an exponential decrease were sometimes observed. These deviations might have been caused by temperature effects and sorption of gases on airborne particulates rather than on the test substrates.

TABLE 5. SUMMARY OF STIRRED CHAMBER LOSSES

Expt. No.	SC	HAP Chemical Name	Deposition Surface	Surface Area (m^2)	Fan Speed (rpm)	SF_6 Loss† (%/h)	HAP Loss† (%/h)	HAP Deposition† (%/h)
1	1	perchloroethylene	cement	10.0	520	3.06 ± 0.16	3.48 ± 0.24	0.42 ± 0.31
	2	perchloroethylene	cement	6.1	520	2.04 ± 0.10	2.40 ± 0.19	0.36 ± 0.27
2	1	perchloroethylene	cement	10.0	520	2.58 ± 0.26	2.93 ± 0.27	0.34 ± 0.35
	2	perchloroethylene	cement	6.1	520	1.20 ± 0.10	1.96 ± 0.08	0.75 ± 0.12
4	1	perchloroethylene	cement	10.0	600	6.17 ± 0.04	6.89 ± 0.17	0.72 ± 0.17
	2	perchloroethylene	cement	6.1	600	3.94 ± 0.10	4.02 ± 0.11	0.08 ± 0.14
6	1	perchloroethylene	tile	6.0	520	3.06 ± 0.09	3.46 ± 0.08	0.41 ± 0.14
7	1	perchloroethylene	tar paper	6.0	520	1.44 ± 0.06	1.92 ± 0.17	0.48 ± 0.14
8	2	perchloroethylene	tile	6.0	520	2.90 ± 0.25	2.88 ± 0.52	-0.02 ± 0.53
9	1	perchloroethylene	tar paper	6.0	520	2.74 ± 0.25	2.80 ± 0.38	0.06 ± 0.42
10	2	perchloroethylene	tile	6.0	600	5.73 ± 0.40	6.89 ± 0.54	1.16 ± 0.61
11	1	perchloroethylene	tar paper	6.0	600	2.73 ± 0.27	4.30 ± 1.32	1.57 ± 0.98
15	1	nitrobenzene	tar paper	6.0	520	4.03 ± 0.38	6.99 ± 3.98	2.96 ± 3.60
16	2	nitrobenzene	tile	6.0	520	3.48 ± 0.19	3.48 ± 1.13	0.01 ± 1.06
17	1	nitrobenzene	tar paper	6.0	520	3.03 ± 0.15	3.73 ± 1.48	0.70 ± 1.27
18	2	nitrobenzene	tile	6.0	520	3.69 ± 0.07	4.88 ± 0.76	1.19 ± 0.69
19	1	nitrobenzene	tar paper	6.0	520	3.56 ± 0.22	4.24 ± 0.76	0.68 ± 0.72

† Tabulated uncertainties represent the 90% confidence interval.

TABLE 6. HAP-DRY DEPOSITION VELOCITIES

Expt. No.	SC	HAP Chemical Name	Deposition Surface	Surface Area (m^2)	Fan Speed (rpm)	HAP Deposition† (%/h)	Deposition Velocity † (cm/sec)
1	1	perchloroethylene	cement	10.0	520	0.42 ± 0.31	$5.2 \pm 3.8 \times 10^{-5}$
	2	perchloroethylene	cement	6.1	520	0.36 ± 0.27	$7.3 \pm 5.5 \times 10^{-5}$
2	1	perchloroethylene	cement	10.0	520	0.34 ± 0.35	$4.2 \pm 4.3 \times 10^{-5}$
	2	perchloroethylene	cement	6.1	520	0.75 ± 0.12	$1.5 \pm 0.2 \times 10^{-4}$
4	1	perchloroethylene	cement	10.0	600	0.72 ± 0.17	$8.9 \pm 2.1 \times 10^{-5}$
	2	perchloroethylene	cement	6.1	600	0.08 ± 0.14	$1.6 \pm 2.8 \times 10^{-5}$
6	1	perchloroethylene	tile	6.0	520	0.41 ± 0.14	$8.4 \pm 2.9 \times 10^{-5}$
7	1	perchloroethylene	tar paper	6.0	520	0.48 ± 0.14	$9.9 \pm 2.9 \times 10^{-5}$
8	2	perchloroethylene	tile	6.0	520	-0.02 ± 0.53	$-0.0 \pm 1.1 \times 10^{-4}$
9	1	perchloroethylene	tar paper	6.0	520	0.06 ± 0.42	$1.2 \pm 8.6 \times 10^{-5}$
10	2	perchloroethylene	tile	6.0	600	1.10 ± 0.61	$2.4 \pm 1.3 \times 10^{-5}$
11	1	perchloroethylene	tar paper	6.0	600	1.57 ± 0.98	$3.2 \pm 2.0 \times 10^{-4}$
15	1	nitrobenzene	tar paper	6.0	520	2.96 ± 3.60	$6.1 \pm 7.4 \times 10^{-4}$
16	2	nitrobenzene	tile	6.0	520	0.01 ± 1.06	$0.0 \pm 2.2 \times 10^{-4}$
17	1	nitrobenzene	tar paper	6.0	520	0.70 ± 1.27	$1.4 \pm 2.6 \times 10^{-4}$
18	2	nitrobenzene	tile	6.0	520	1.19 ± 0.69	$2.5 \pm 1.4 \times 10^{-4}$
19	1	nitrobenzene	tar paper	6.0	520	0.68 ± 0.72	$1.4 \pm 1.5 \times 10^{-4}$

† Tabulated uncertainties represent the 90% confidence interval.

SECTION 5

DATA INTERPRETATION AND GENERALIZATION

DATA INTERPRETATION

Using Equation 6, deposition velocities were calculated from the HAP loss rates listed in the last column in Table 5. For these calculations, HAP and SF_6 leak rates were assumed identical, and deposition in the SC to surfaces other than the selected deposition substrate was assumed negligible (see Appendix B). Because the deposition velocities were low and the operating range of the fan speed in the SC was small, changes in deposition velocities as a function of fan wind speed could not be determined. Most experiments were conducted at the maximum usable fan speed of 520 rpm. It is unknown whether deposition velocities would have increased if fan speed could have been increased. Hence, the deposition velocities reported may not correspond to the inverse of the substrate resistance. Results are summarized in Table 6. The calculated HAP dry-deposition velocities ranged from zero to about 6×10^{-4} cm/s. All of the values are relatively small, and given the appropriate 90% confidence limits, many of the deposition velocities are not significantly different from zero.

These HAP dry-deposition velocities are near the lower limit (10^{-4} cm/s) for gases shown in Table 2 (except for the noble gas krypton and the less than 10^{-4} cm/s for CCl_4). The relatively low HAP dry-deposition velocities possibly were caused by differences in the substrate (building materials versus vegetative canopies), or result because organic gases deposit less rapidly than inorganic gases. Further research is needed to clarify these possibilities.

APPLICATION OF MEASURED DRY-DEPOSITION VELOCITIES

The HAP dry-deposition velocities listed in Table 6 are assumed to reflect only the substrate resistance to mass transfer. However, dry-deposition removal rates from the atmosphere are a function of gas properties, deposition substrates, and meteorological parameters. To simplify analysis of the various processes contributing to transfer of material to the surface, HAP

materials are considered to be transported across several layers, each of which has a characteristic resistance, r, to vertical transfer. Because the layers are horizontal, the resistances are in series and the relationship between the resistances and the net deposition velocity is

$$V_d = (r_a + r_s + r_g)^{-1} \tag{8}$$

where r_a is the aerodynamic resistance, r_s is the surface resistance, and r_g is substrate resistance.

The aerodynamic resistance, r_a, is solely a function of vertical transport by turbulent atmospheric eddies. Thus, it depends only on the properties of the atmosphere and the aerodynamic roughness of the surface. This turbulent transport of material has been found to be similar to that of heat (5), which is well known from micrometeorological observations (6). The r_a is inversely proportional to the atmospheric turbulent mixing. Its relative importance to r_s and r_g depends on the height for which the deposition velocity is defined. For a height of 1 m and a moderately rough surface, $r_a = 10/u_*$, where u_* is the friction velocity, which is a measure of atmospheric mixing.

The surface resistance, r_s, accounts for transfer across the thin layer of air in contact with the surface elements. Since atmospheric mixing becomes small at the surface, r_s depends also on molecular diffusion and hence on the properties of the test gas. The surface resistance is commonly expressed as

$$r_s = B^{-1}/u_* \tag{9}$$

where B^{-1} is an inverse Stanton number (7). The surface resistance has been studied extensively, but is less well known than the aerodynamic resistance. Wesely and Hicks (8) assume that B^{-1} is proportional to $(K/D)^{2/3}$ where K is the thermal diffusivity of air and D is the molecular diffusivity of the test gas. For SO_2, $B^{-1} = 6.5$, and hence r_s may be comparable to r_a.

The substrate resistance, r_g, is least well known and reflects the processes by which the test gas is captured and retained by the substrate. Because this resistance is highly dependent on the properties of the test gas and the deposition substrate, the experimental design of this project emphasized its measurement. The atmosphere in the SC was mixed in order to reduce the aerodynamic and surface resistances (especially since deposition rates were so small) so that the measured deposition velocities reflect chiefly the substrate resistance. As the SC atmosphere is mixed and the aerodynamic resistance is reduced, the concentration in the chamber becomes uniform. Neglecting the aerodynamic resistance,

$$v_{ds} = (B^{-1}/u_* + r_g)^{-1}. \qquad (10)$$

As the mixing, and hence u_*, is increased, the surface resistance is reduced and the deposition velocity increases. When the measured deposition velocity becomes independent of the mixing, it reaches an upper limit equal to the inverse of the substrate resistance. The net deposition velocity, which is required for air-quality modeling, can then be recovered by applying Equation 8 with the measured value for r_g and known relationships for r_a and r_s. As previously indicated, dry-deposition velocities were near detection limits at the maximum fan speed.

SECTION 6

DEPOSITION MODELING

The deposition model developed under this project and the concurrent one, Hazardous Air Pollutants: Wet Removal Rates and Mechanisms, is called MPADD. MPADD simulates the behavior of a single or multicomponent plume of airborne material as it is transported, reacted, scavenged, and dry-deposited downwind. The code is intended to provide a convenient and useful method for practical assessment of the behavior of airborne hazardous air pollutants.

MPADD is a somewhat distant descendent of the reactive plume-scavenging model, SMICK (9), although these are totally separate codes and there is little resemblance between the two. MPADD represents a substantial advancement beyond SMICK; in particular,

- MPADD uses a newer and much more efficient procedure for numerical integration of the model's governing equations. This substantially decreases computer-time requirements for code execution, especially in cases involving stiff differential equations.
- MPADD includes dry deposition as well as wet deposition.
- MPADD accounts for gaseous plume depletion.
- MPADD is much more streamlined and modularized, allowing faster operation and enhanced versatility.

The above features represent considerable improvements over MPADD's predecessors, and regardless of the nature of the source configuration (e.g., tall stacks, urban areas, disposal sites, ...), the MPADD framework produces a much more convenient method for general plume scavenging and deposition calculations. MPADD essentially renders SMICK obsolete and should be employed for all situations where SMICK formerly would have been used.

A detailed summary of MPADD is included in the final report of the wet deposition project (1), and a complete description with computer listings can be found in the user's manual, submitted with that report. Here we will only

outline the overall operation of the model and provide a brief summary of the dry deposition components.

Macroscopic features of the deposition model are summarized in Figure 2. Here the ensemble of gas-phase pollutants is emitted as a plume (or composite of individual plumes) from some sort of generalized source region, whereupon they experience advection, mixing, possible chemical reaction, and dry and wet deposition. The dry-deposition flux is calculated for each pollutant as the product of its gas-phase concentration at ground level and its dry-deposition velocity. Wet removal is computed by allowing precipitation to fall through the plume over trajectories determined by the raindrops' fall speeds and the mean wind. Typically the raindrop spectrum is discretized into a number of size categories, and total delivery at a receptor point (XG, YG, ZG) is computed by evaluating the composite of individual contributions over this spectrum. The code's operation is based on the establishment of some arbitrary datum point ($x = 0$, $y = 0$, $z = 0$). For symmetric plumes the plane defined by $y = 0$ normally would define the centerplane of the plume, but this is not absolutely necessary. Similarly, $x = 0$ and $z = 0$ usually relate strongly to the source location, but considerable latitude can be given regarding this choice. For the specific plume model employed by the present projects (which is indeed symmetric about the y axis), $y = 0$ is taken to coincide with the centerplane; $x = 0$ and $z = H$ are taken as the coordinates of the farthest upwind extremity of the source. Normal operation of the code is to initially advance downwind by a distance DX(1), numerically integrating the dry-deposition flux in the downwind direction to account for dry removal in that increment. An array of lateral wet deposition values (spaced at interavals DY) is then computed at the current x-location, and these values are integrated numerically to estimate plume depletion arising from wet deposition to this point. At each downwind distance the gas-phase plumes are modified by adjusting their effective source terms to account for upwind removal. Upon completion of this step, the code advances the increment DX(2) to a new downwind distance, dry and wet deposition are calculated for that increment, and the process is repeated until a normal exit from the code is accomplished.

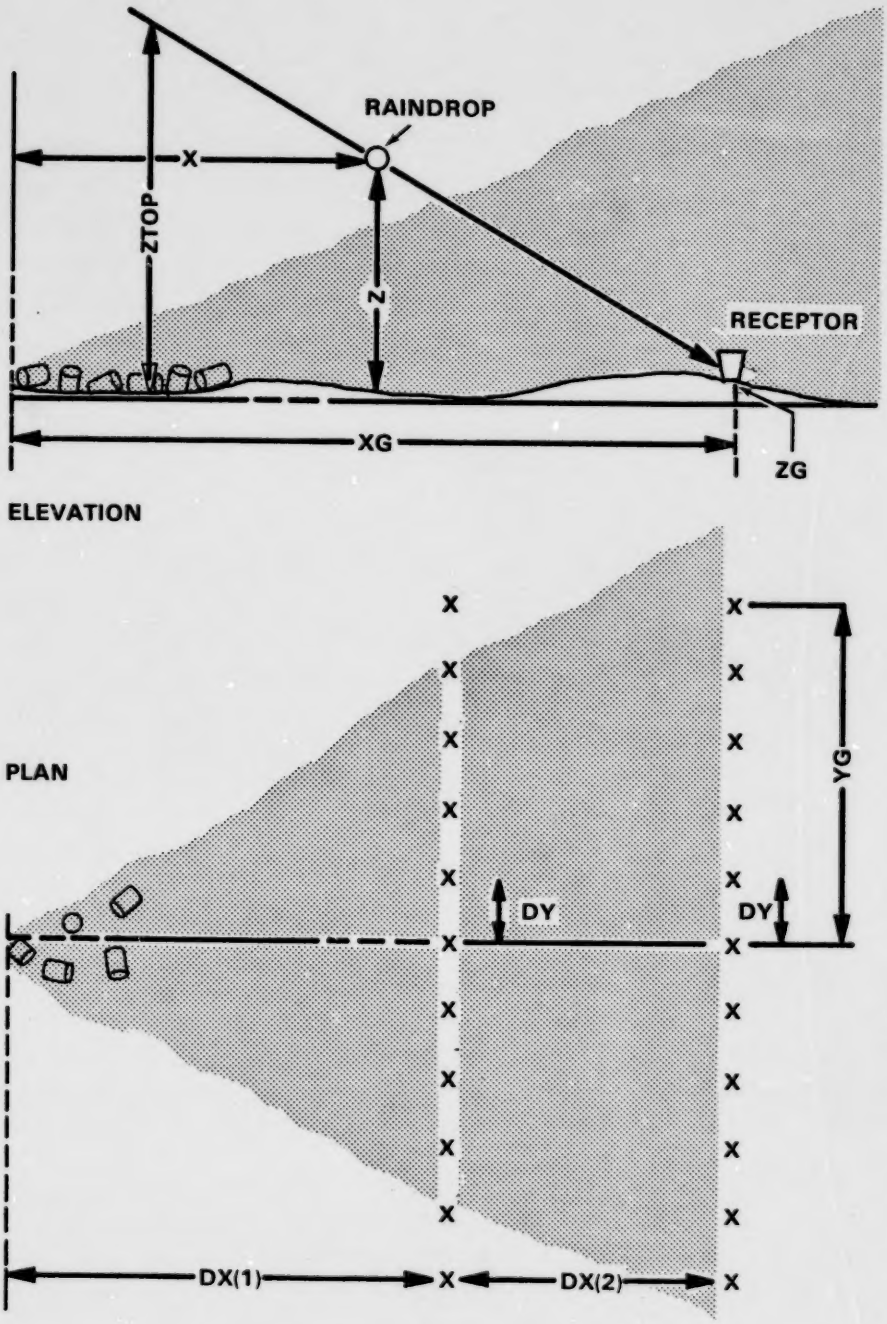

Figure 2. Schematic elevation and plans views of model layout

The plume submodel currently used is the standard Gaussian plume diffusion model. This selection was made on the basis of computational simplicity, scientific credibility, and general applicability to problems associated with hazardous air pollutants. Plume depletion by dry deposition is calculated with an adaptation of subroutine RCONAD from the EPA Gaussian plume computer code PAL-DS (10). The RCONAD estimates of plume depletion compare favorably with those of Horst's surface depletion model (11), an exact solution for depletion of the Gaussian plume by dry deposition. It should be emphasized that the particular plume submodel chosen is only one of a wide variety of possible candidates and can be replaced at the user's discretion with any plume model satisfying modest calculational requirements.

The subroutine for calculating the gas-phase plume, in current applications, determines the gas-phase concentrations c_{gas} and dry deposition fluxes vdc_{gas} using the modified Gaussian plume formula,

$$c_{gas}(x,y,z) = \frac{Q(x)\ \exp\left[-y^2/2\sigma_y^2\right]}{\sqrt{2\pi u\sigma_y}}\ \frac{RCZ}{HF} \qquad (11)$$

where Q(x) is the depleted source strength that has been reduced to account for the loss of mass by dry and wet deposition. RCZ and HF are the ground-level, crosswind-integrated concentration and the total horizontal flux of gas-phase pollutant calculated by subroutine RCONAD. In the limit when pollutant dry deposition and settling velocities are equal to zero,

$$RCZ/HF = \left\{\exp\left[-(H-z)^2/2\sigma_z^2\right] + \left[\exp -(H+z)^2/2\sigma_z^2\right]\right\}/\sqrt{2\pi\sigma_z} \qquad (12)$$

and the equation for $c_{gas}(x,y,z)$ reduces to the standard Gaussian plume formula.

The crosswind and vertical plume standard deviations, σ_y and σ_z, are functions of downwind distance and atmospheric stability calculated by

functions SIGMAY and SIGMAZ. For area sources, σ_y is calculated with a virtual point source located at a distance XUPW upwind of the area source, to account for the initial width of the plume. If the half-width of the area source in the crosswind direction is HW, it is suggested that $2\sigma_y$ (XUPW) = HW.

RCONAD calculates the normalized, crosswind-integrated gas-phase pollutant concentration uc^{-y}_{gas}/Q and the normalized, total horizontal pollutant flux (the vertical integral of uc^{-y}_{gas}/Q) for a Gaussian plume depleted by dry deposition. RCONAD uses diffusion-deposition algorithms that are based on analytical solutions of a gradient-transfer model for dry deposition of both gaseous and particulate pollutants from a plume (12). For use in MPADD, the PAL-DS subroutine RCONAD has been modified by eliminating the consideration of limited vertical mixing and by adding the calculation of the total horizontal flux of the depleted plume. The horizontal flux is required by the plume subroutine to force the RCONAD model to conserve mass and thus enable additional plume depletion by wet deposition.

For each gaseous species IGAS, the dry deposition subroutine calculates the plume depletion by dry deposition from X1 to X2 and increases the cumulative depletion from its input value at X1 to its output value at X2,

$$DDD_{X2} = DDD_{X1} + \int_{X1}^{X2} v_d c^{-y}_{gas}(x,z=0)\ dx \quad .X1 \qquad (13)$$

Here v_d is the dry-deposition velocity and c^{-y}_{gas} is the ground-level, crosswind-integrated gaseous concentration. The integrand, normalized by the local depleted source strength, is calculated by calling the plume subroutine.

The depletion integral is calculated by dividing the interval from X1 to X2 into roughly 20 logarithmically spaced increments per decade and integrating numerically by Simpson's method,

$$DDD_{i+2} = DDD_i + \left[Q_i \times X_i \times XDINT_i + 4 \times Q_{i+1} \times X_{i+1} \times XDINT_{i+1} + Q_{i+}{}^2 \times X_{i+2} \times XDINT_{i+2}\right] \times (\Delta \ln X)/3 \qquad (14)$$

Here Q_i are the depleted source strengths,

$$Q_i = Q_o - WDD_{X1} - DDD_i = QDPL_{X1} - DDD_i$$

$$Q_{i+1} = QDPL_{X1} - DDD_{i+1} \simeq QDPL_{X1} - (W1 \times DDD_i + W2 \times DDD_{i+2})$$

$$Q_{i+2} = QDPL_{X1} - DDD_{i+2} \quad .$$

REFERENCES

1. Dana, M. Terry, R. N. Lee and J. M. Hales. Hazardous Air Pollutants: Wet Removal Rates and Mechanisms. DW930197-01-1, draft final report, U.S. Environmental Protection Agency, Office of Research and Development, Research Triangle Park, North Carolina, October 1983.

2. Sehmel, G. A. Particle and Gas Dry Deposition: A Review. Atmos. Environ., 14:983-1011, 1980.

3. Cupitt, L. T. Fate of Toxic and Hazardous Materials in the Air Environment, Project Summary, EPA-600/S3-80-084. U.S. Environmental Protection Agency, Research Triangle Park, North Carolina, December 1980.

4. Fox, D. L., J. D. Sickles, M. R. Kuhlman, P. C. Reist and W. E. Wilson. Design and Operation Parameters for a Large Ambient Aerosol Chamber. J. Air. Poll. Control Assoc., 25:1049-1053, 1975.

5. Droppo, J. G. and J. C. Doran. Experimental Constraints in Micrometeorological Gaseous Pollutant Fluxes, in: Precipitation Scavenging, Dry Deposition, and Resuspension, H. R. Pruppacher, R. G. Semonin, and W. G. N. Slinn, eds. 1983 pp. 807-815.

6. Businger, J. A., J. C. Wyngaard, Y. Izumi and E. F. Bradley. Flux-Profile Relationship in the Atmospheric Surface Layer. J. Atmos. Sci., 28:181-189, 1971.

7. Owen, P. R. and W. R. Thomson. Heat Transfer Across Rough Surfaces. J. Fluid Mech., 15:15, 1963.

8. Wesely, M. L. and B. B. Hicks. Some Factors that Affect the Deposition Rates of Sulfur Dioxide and Similar Gases on Vegetation. J. Air. Poll. Control Assoc., 27:1110-1116, 1977.

9. Drewes, D. R. and J. M. Hales. SMICK-A Scavenging Model Incorporating Chemical Kinetics. Atmos. Environ., 16:1717-1724, 1982.

10. Rao, K. S. and H. F. Snodgrass. PAL-DS Model: The PAL Model Including Deposition and Sedimentation - User's Guide. U.S. Environmental Protection Agency, Research Triangle Park, North Carolina, 1981, 40 pp.

11. Horst, T. W. A Surface Depletion Model for Deposition from a Gaussian Plume. Atmos. Environ., 11:41-46, 1977.

12. Rao, K. S. Analytical Solutions of a Gradient-Transfer Model for Plume Deposition and Sedimentation. ERL ARL-109, NOAA Air Resources Laboratories, Silver Spring, Maryland, 1981, 75 pp.

APPENDIX A

ANALYTICAL TECHNIQUES

All analyses were conducted using electron capture gas chromatography. Volatile species were removed from the SC by syringe withdrawal through Teflon® coated septa. The syringe was filled by slowly withdrawing the plunger. This sample was then expelled without removing the syringe needle from the sampling port and the syringe filled a second time for transfer to the gas sampling valve (GSV) of the gas chromatograph. A 10-cc gas-tight syringe (Teflon plunger tip) with a Teflon valve was initially used in sample transfer, but was abandoned in favor of a 30-cc all-glass syringe as a result of tests which demonstrated a significant memory effect in the 10-cc syringe when used with perchloroethylene. In contrast, an all-glass syringe was shown to be free of memory effects and demonstrated excellent sample storage properties.

Replicate analyses in which samples were stored by inserting the syringe needle in a rubber septum showed no change in concentration over a period of up to 30 min. In all chamber tests samples were withdrawn from sampling ports other than those used to introduce hazardous air pollutants (HAPs) or SF_6. This practice avoided the possible bias associated with exposure to a septum that had experienced relatively high concentrations of these materials. As an added precaution the syringe was flushed with outside air between samples and room air was occasionally analyzed to evaluate the potential for positive interference caused by HAP memory in the transfer syringe or GSV. In all transfer operations the syringe was sealed by inserting the needle in a rubber septum and injected for analysis within 5 min of collection.

® Registered trademark of the DuPont Company, Wilmington, Delaware.

Sulfur hexafluoride was measured using a Systems, Science and Software[a] Model 215AUP SF_6 monitor with a 2.5-ft x 1/4-in. outside-diameter copper column packed with aluminum, and a 2-cc sample loop for sample injection. Ultrapure nitrogen served as the carrier gas for transport of the sample through the column to the detector [tritiated titanium electron capture detector (ECD)]. Both the column and detector operate at ambient temperature. Previous experience with this analyzer has demonstrated linear detector response to well beyond 1000 ppt. During the course of the chamber experiments single-point calibration checks were made at approximately 1-h intervals to document stable detector performance. A 310-ppt primary standard SF_6 in ultrapure air mixture obtained from Scott-Marrin, Inc.[b] was used for all calibration checks. During all experiments, analyzer response to the calibration standard showed a precision of better than 5%. The sample chromatogram was recorded using a strip chart recorder and the SF_6 concentrations quantified by measuring peak height.

Perchloroethylene was measured using a Hewett Packard[c] Model 5736 gas chromatograph equipped with a Ni^{63} frequency-modulated electron capture detector. Perchloroethylene was isolated from other sample components by using a 4-ft x 2-mm-ID glass column packed with 2 percent OV-101 on 100/120 W-HP. The carrier gas (10% methane in argon) flow rate was adjusted to 46 cc/min with the column and detector temperatures at 40°C and 200°C, respectively. Chromatograms were recorded using a Hewett Packard Model 3380A Integrating Recorder and concentrations determined from peak area.

Standard perchloroethylene in air samples were generated with a AID (Analytical Instrument Development, Inc.)[d] permeation tube maintained at a constant temperature in an AID Model 309 Gas Calibrator with compressed air (breathing quality) as the diluent. Multipoint calibration checks were conducted before the start of the series of chamber experiments to document

---

(a) Systems Science and Software, LaJolla, California.
(b) Scott-Marrin, Inc., Riverside, California.
(c) Hewett-Packard Inc., Avondale, Pennsylvania.
(d) Analytical Instrument Development, Inc., Avondale, Pennsylvania.

the linearity of detector response. Single-point calibration checks were then included at approximately 1-h intervals during individual experiments to illustrate stable detector operation and quantify response. Replicate analyses of the standard during individual runs showed a precision of less than 7% at the 98.6 ppb level.

The lower volatility and somewhat higher detection limits obtainable for nitrobenzene with either the ECD or nitrogen-phosphorus selective flame ionization detector option required a different approach to measuring chamber concentrations. The method adopted was that used to survey workplace exposure levels. Adsorption tubes (silica gel, SKC[a] Catalog No. 226-10) were connected to 1/4-in.-OD Teflon tubing from the bulkhead union in the chamber wall and the union in turn to 1/8-in.-OD Teflon tubing (25 cm) in the chamber interior. Chamber air was then pulled through the adsorption tube at approximately 90 cc/min using a personnel air sampling pump (Supelco[b], Catalog No. 2-2957). Sampling times varying from 15 to 30 minutes resulted in the concentration of nitrobenzene from 1.35 to 2.70 liters of chamber air. This generally provided sufficient analyte to permit quantitative detection and as many as ten 30-min samples represented only a small fraction (less than 1% of the total chamber volume. The nitrobenzene sampling times reported in Tables D-15 through D-19 in Appendix D correspond to the midpoint in the respective sample collection periods.

After sample collection, adsorbent tubes were capped and stored at approximately 4°C until ready for laboratory analysis. Preparation for analysis consisted of desorption with 1.0 ml of methanol and 30 min of mixing using a sample agitator, after which nitrobenzene was measured using electron capture gas chromatography. Two microliter samples of the extract were injected for analysis using the solvent flush method and nitrobenzene quantified from peak area using a Hewett-Packard Model 3380A

(a) SKC, Inc., Fullerton, California.
(b) Supelco, Inc., Bellefonte, Pennsylvania.

integrating recorder. Sample components were separated on a 6 ft x 1/8-in.-OD stainless steel column containing 10 percent OV-17 on 80/100 W-HP. The injector, column, and detector were at 100, 150, and 250°C, respectively. Detector response was calibrated with standards prepared by serial dilution of a nitrobenzene in ethanol stock solution with methanol. Standards in the 10 to 100 ng/ml range were interspersed with chamber samples to document stable detector performance.

APPENDIX B

TESTS OF STIRRED CHAMBER LEAKAGE AND WALL LOSS

The two stirred chambers (SCs) were tested for leaks and HAP wall loss. The two SC's were checked for leaks with SF_6 tracer gas before the experiments with hazardous air pollutants (HAP) were begun. Sulfur hexafluoride concentrations were normalized using the SF_6 concentration at the beginning of the experiment. As shown in Figure B-1, leakage rates were about 1 %/h. Leakage rates tended to increase during the actual HAP experiments, but were always evaluated. When they seemed too large, further effort was directed to find and eliminate sources of leaks.

The HAP wall losses to empty SCs were evaluated immediately before and after the series of experiments using perchloroethylene and cement as a deposition substrate. Initially, HAP losses were not measurable (i.e., loss rates were identical for both HAP and SF_6). After the perchloroethylene dry-deposition experiments were completed, HAP wall losses were reevaluated in experiment number 5. Wall losses increased. However, wall losses evaluated in experiment number 5 are considered unrealistic in comparison to the prior experiments. Losses may have increased because residual cement particles may have remained on the SC floor after the cement blocks were removed and the chamber cleaned of larger cement particles. Fine cement particles may have remained on the floor. This would provide increased surface area for deposition If this is the case, these residual particles did not bias the subsequent experiments since the SC floor was covered with either tile or tar paper.

For experiment number 5, losses for both HAP and SF_6 are shown graphically in Figures B-2 and B-3, are listed in Tables B-1 and B-2, and are summarized in Table B-3. The HAP wall losses had increased to 1.51 %/h in SC number 1, and to 0.59 %/h in SC number 2. These wall losses were greater than the HAP deposition losses to the cement. In SC number 1, the HAP deposition

losses to cement (see Table 5) were 0.42, 0.03, and 0.08 %/h. Similarly in SC number 2, the HAP deposition losses to cement were 0.36, 0.35, and 0.08 %/h, while the wall loss to the empty SC in experiment 5 was 0.59 %/h.

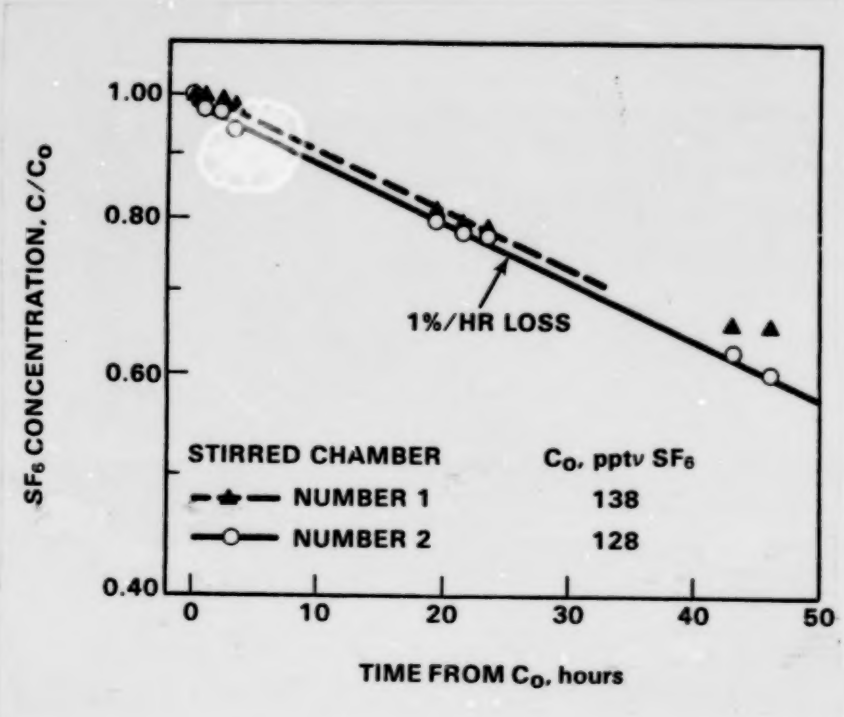

Figure B-1. SF_6 Concentration decrease with time in empty stirred chambers.

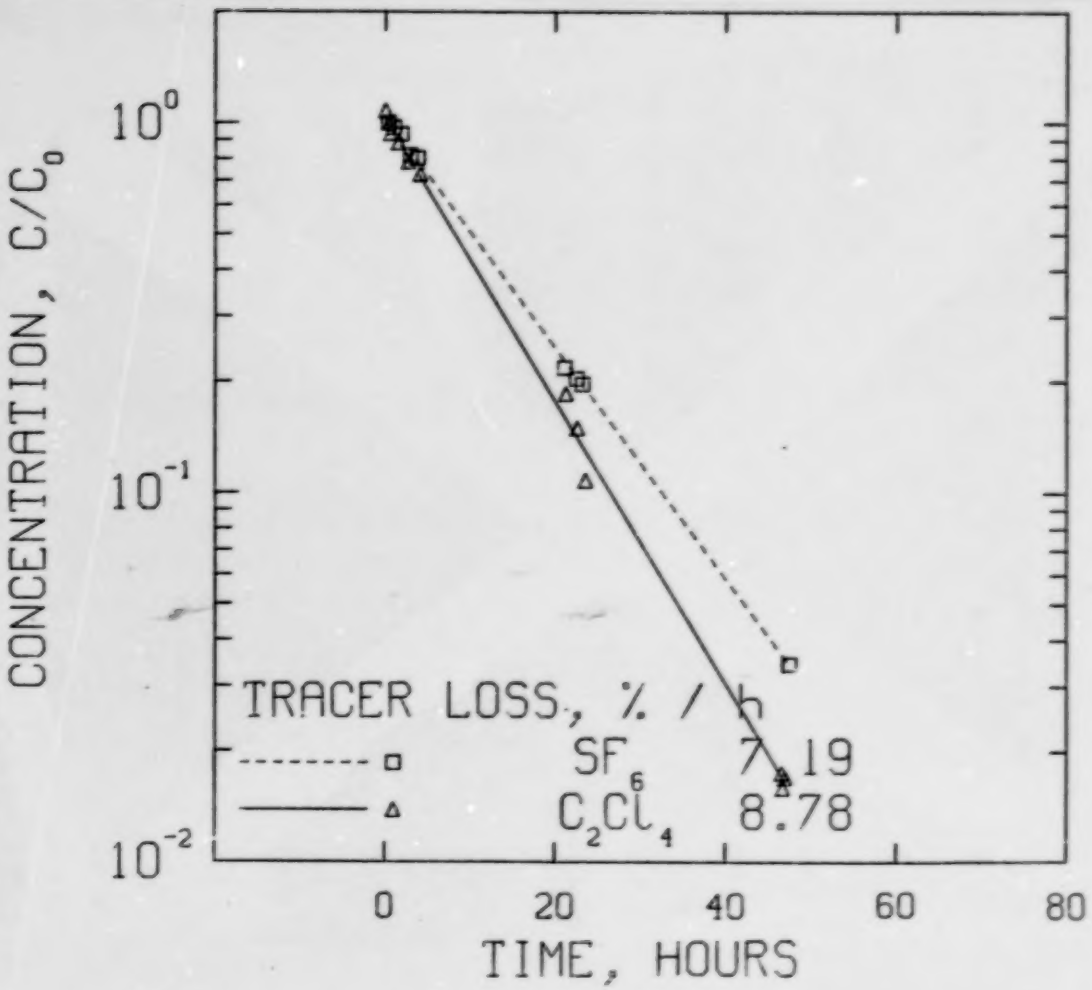

Figure B-2. Run 5-1: Perchloroethylene and SF_6 tracer gas concentration decreases for empty SC number 1.

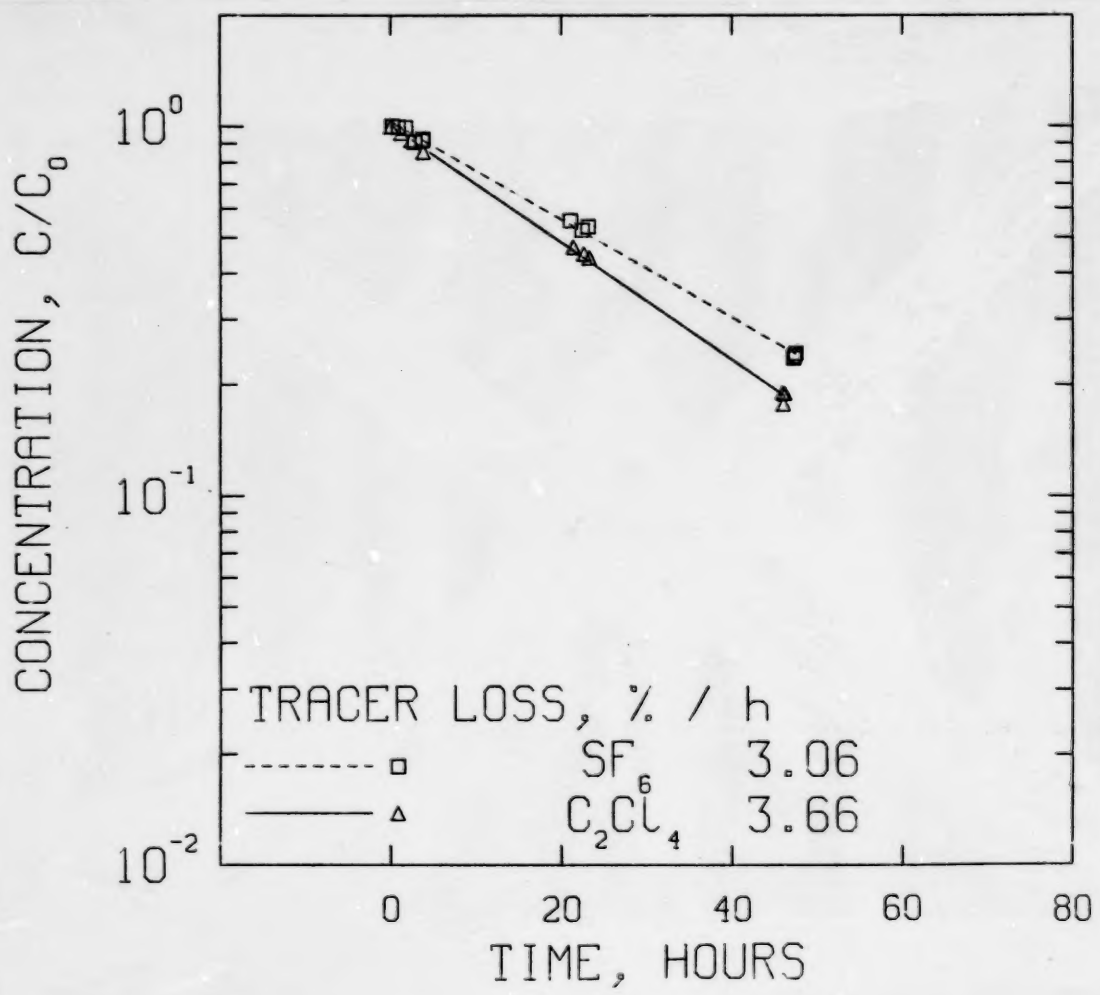

Figure B-3. Run 5-2: Perchloroethylene and SF_6 tracer gas concentration decreases for empty SC number 2.

TABLE B-1. RUN 5-1: PERCHLOROETHYLENE AND SF_6 TRACER GAS CONCENTRATION DECREASES FOR AN EMPTY SC

HAP sampling data			SF_6 sampling data		
Day	Time (h.min)	Concentration (ppm)	Day	Time (h.min)	Concentration (ppm)
25	12.00	70.	25	12.22	860*
25	12.26	64.9*	25	12.59	836
25	12.36	60.7	25	13.54	801
25	13.30	57.4	25	14.58	703
25	14.44	51.	25	15.46	692
25	16.06	47.2	25	15.49	692
26	9.17	12.	26	9.09	187
26	10.38	9.7	26	10.33	175
26	11.35	7.	26	11.13	169
27	10.36	1.13	27	11.31	29.5
27	10.43	1.03	27	11.35	29.5
27	11.00	1.1			

*C_o for normalizing in figures.

TABLE B-2. RUN 5-2: PERCHLOROETHYLENE AND SF_6 TRACER GAS CONCENTRATION DECREASES FOR AN EMPTY SC

HAP sampling data			SF_6 sampling data		
Day	Time (h.min)	Concentration (ppm)	Day	Time (h.min)	Concentration (ppm)
25	12.10	117.7*	25	12.24	1381*
25	13.23	112.9	25	13.04	1375
25	14.35	107.9	25	13.57	1369
25	16.00	100.4	25	15.01	1252
26	9.33	55.4	25	15.52	1264
26	10.47	53.1	25	15.58	1276
26	11.24	51.8	26	9.13	767
27	10.06	22.3	26	10.36	724
27	10.10	20.8	26	11.17	739
27	10.23	22.2	27	11.26	325
			27	11.28	330
			27	11.40	335

*C_o for normalizing in figures.

TABLE B-3. EMPTY STIRRED CHAMBER LOSSES

Exp. num.	SC	HAP compound	Fan speed (rpm)	SF_6 loss (%/h)	HAP loss (%/h)	HAP deposition (%/h)
5	1	perchloroethylene	520	7.19	8.78	1.51
	2	perchloroethylene	520	3.06	3.66	0.59

APPENDIX C

HAP AND SF_6 CONCENTRATION LOSS RATES

Stirred chamber loss rates are reported for seventeen experiments made to determine hazardous air pollutant (HAP) dry-deposition removal rates. These experiments were made during runs (C-1 through C-17). However, some experimental results are not reported because of either low concentrations or analytical problems.

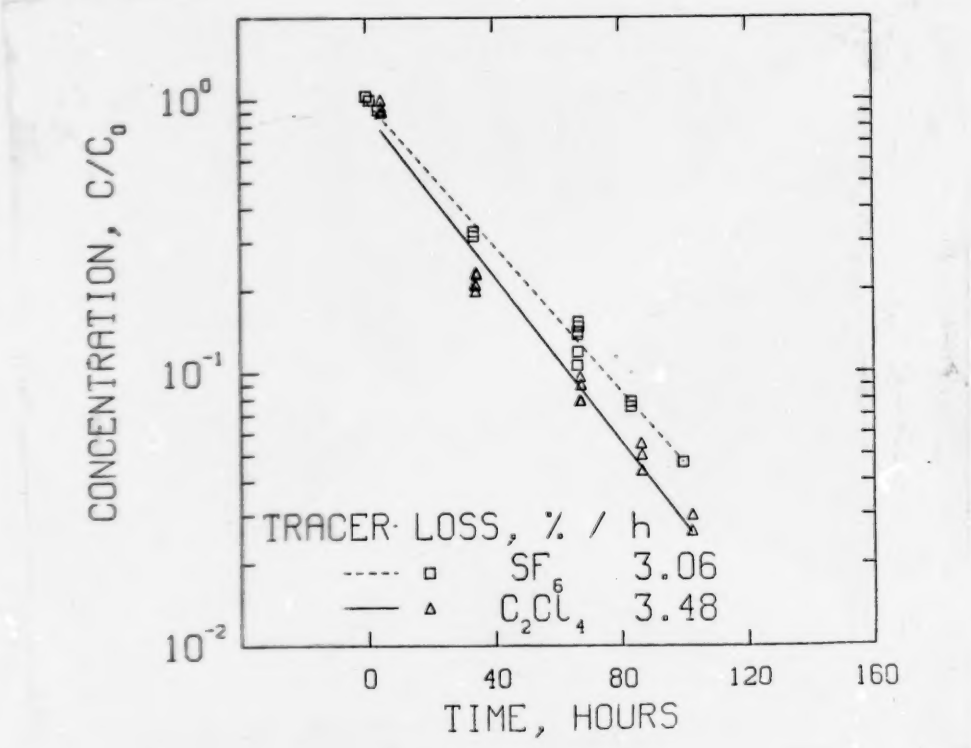

Figure C-1. Run 1-1: Perchloroethylene and SF_6 tracer gas concentration decreases for 10.0 m^2 of cement block deposition surface.

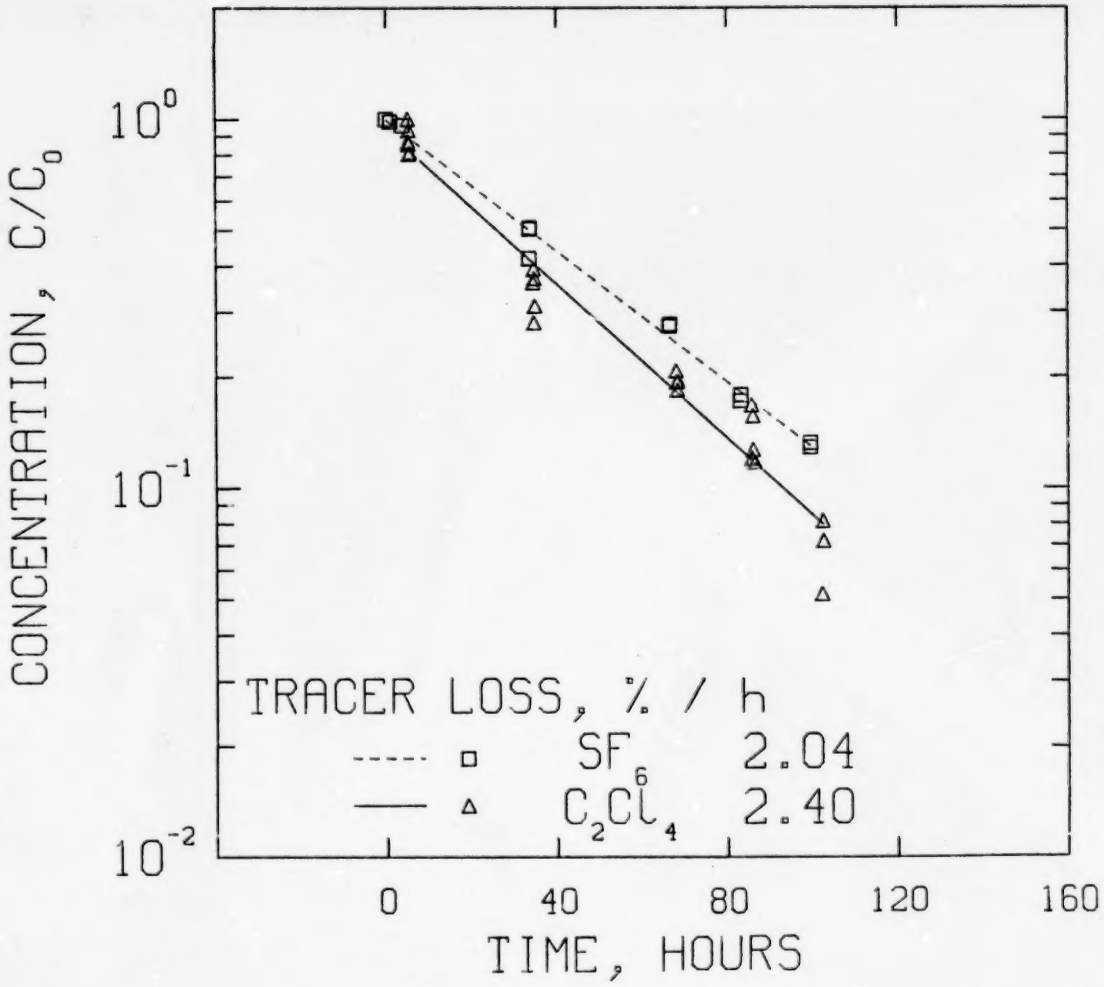

Figure C-2. Run 1-2: Perchloroethylene and SF_6 tracer gas concentration decreases for 6.1 m^2 of cement block deposition surface.

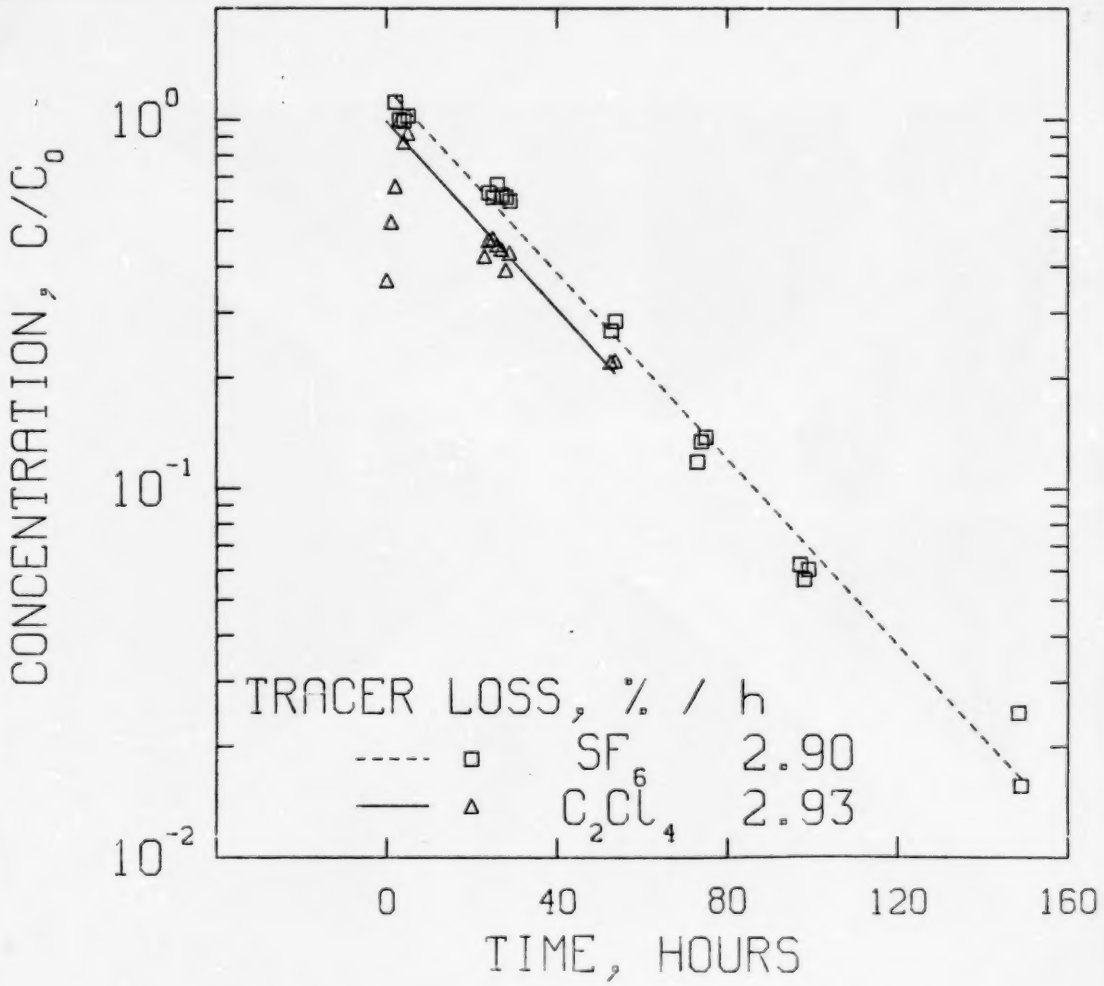

Figure C-3. Run 2-1: Perchloroethylene and SF_6 tracer gas concentration decreases for 10.0 m^2 of cement block deposition surface.

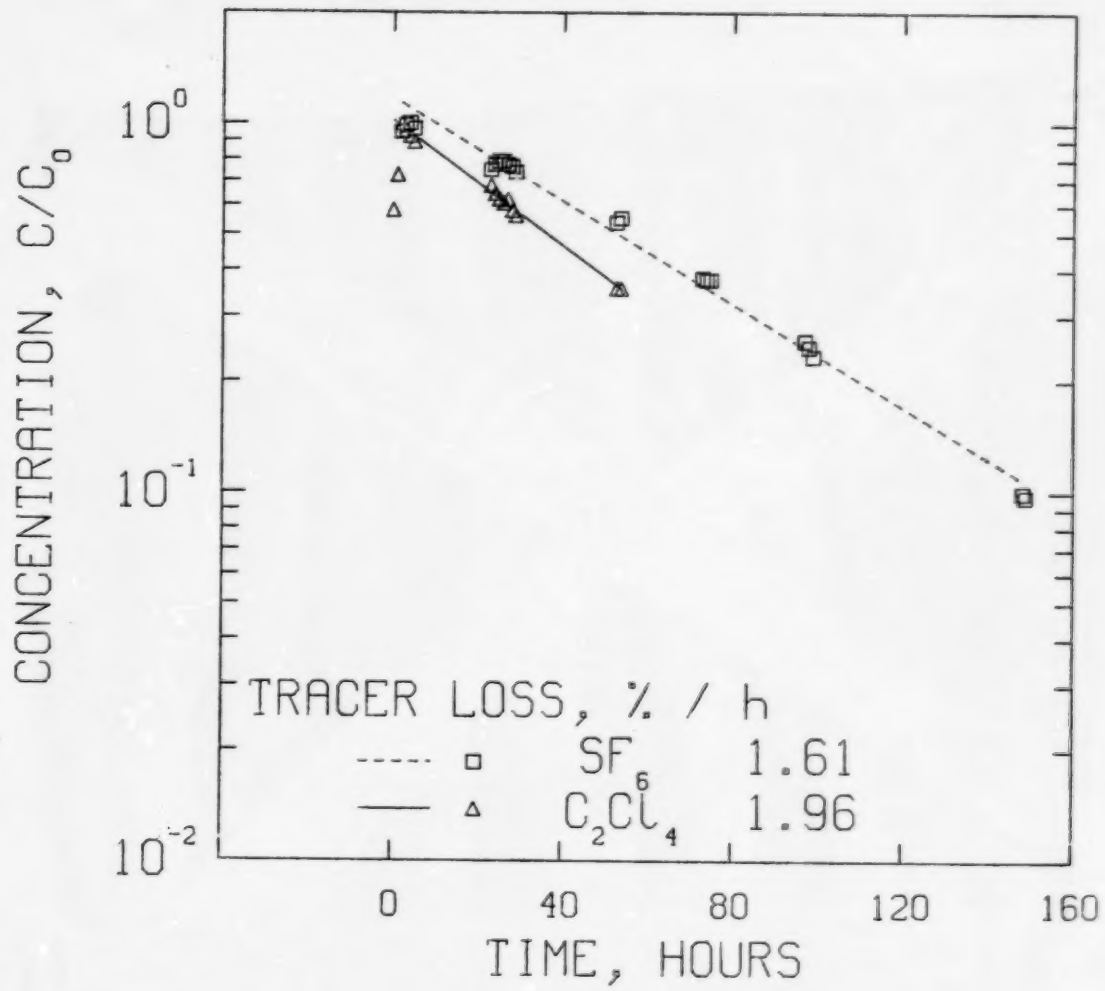

Figure C-4. Run 2-2: Perchloroethylene and SF_6 tracer gas concentration decreases for 6.1 m^2 of cement block deposition surface.

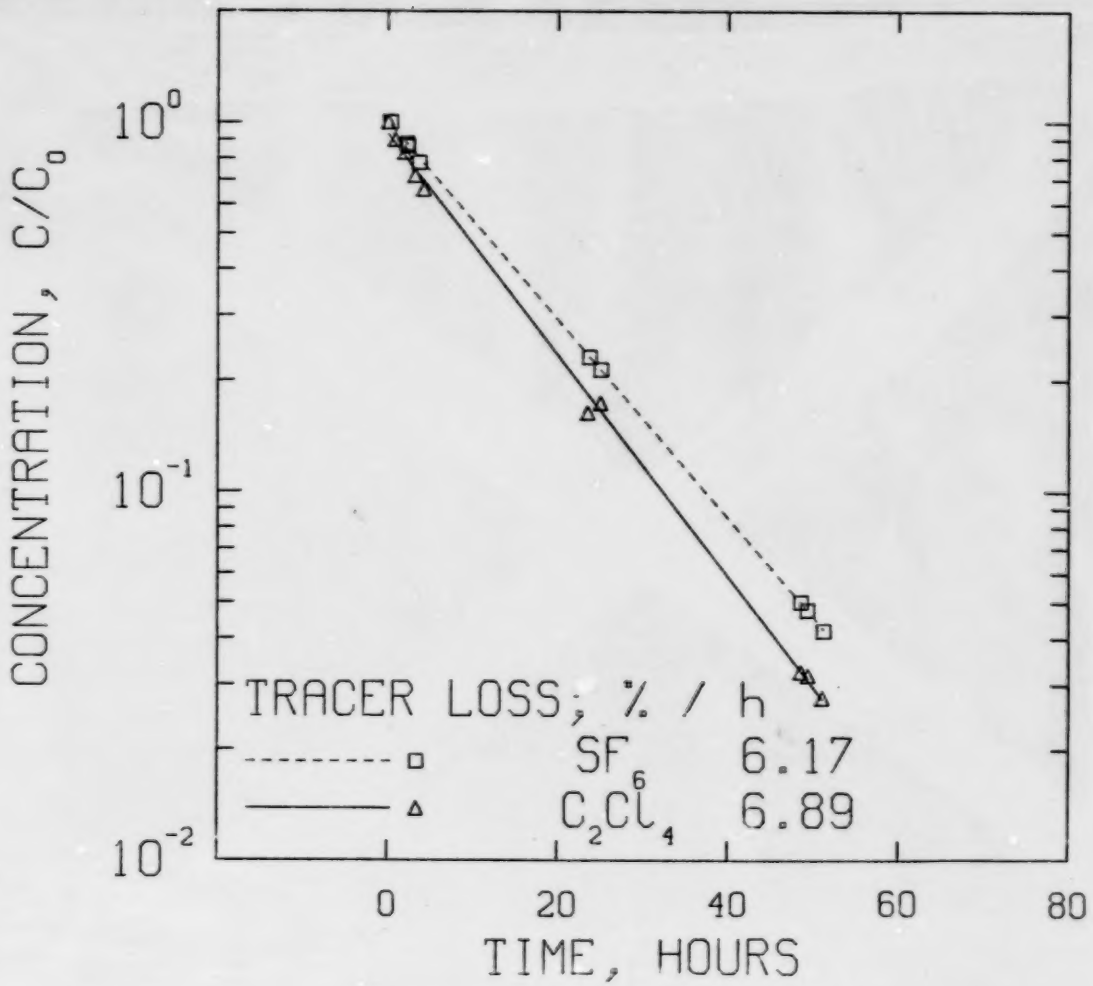

Figure C-5. Run 4-1: Perchloroethylene and SF_6 tracer gas concentration decreases for 10.0 m^2 of cement block deposition surface.

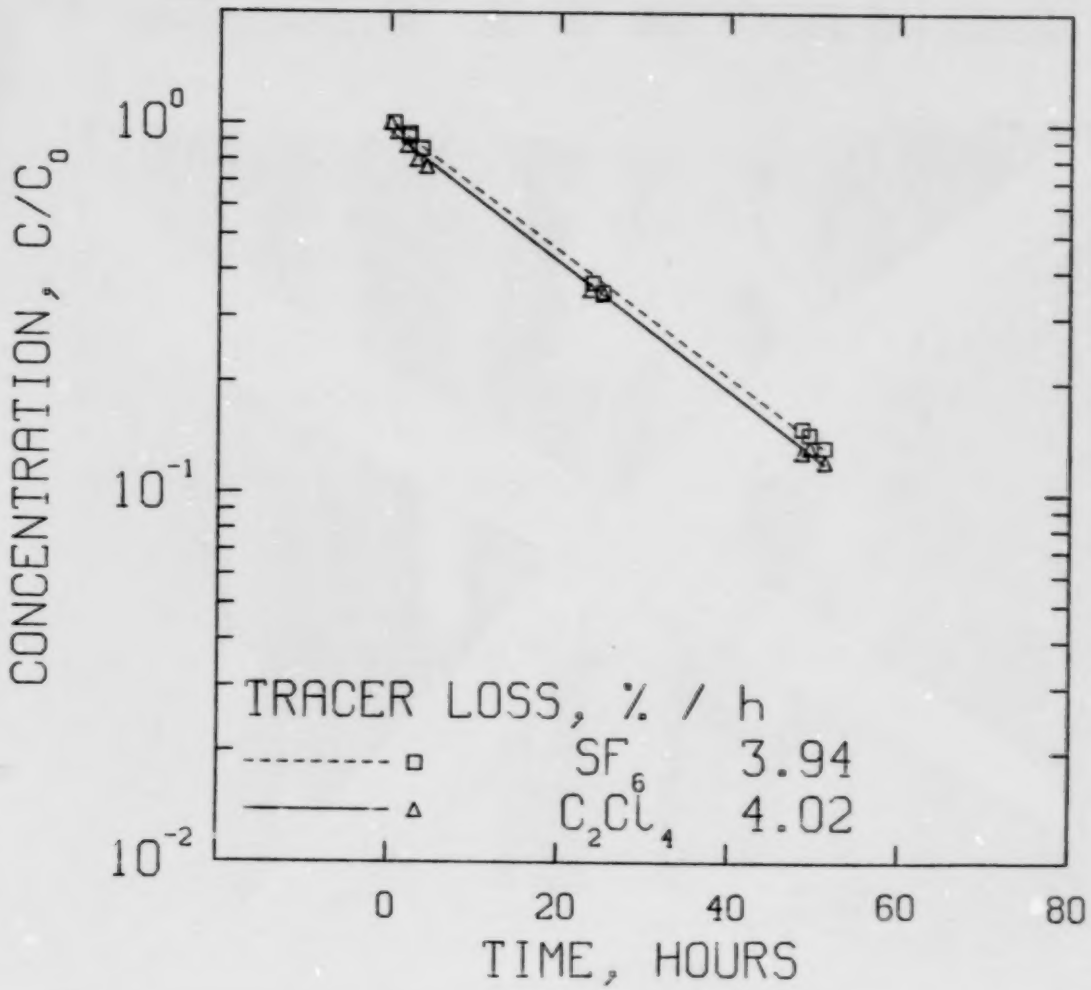

Figure C-6. Run 4-2: Perchloroethylene and SF_6 tracer gas concentration decreases for 6.1 m^2 of cement block deposition surface.

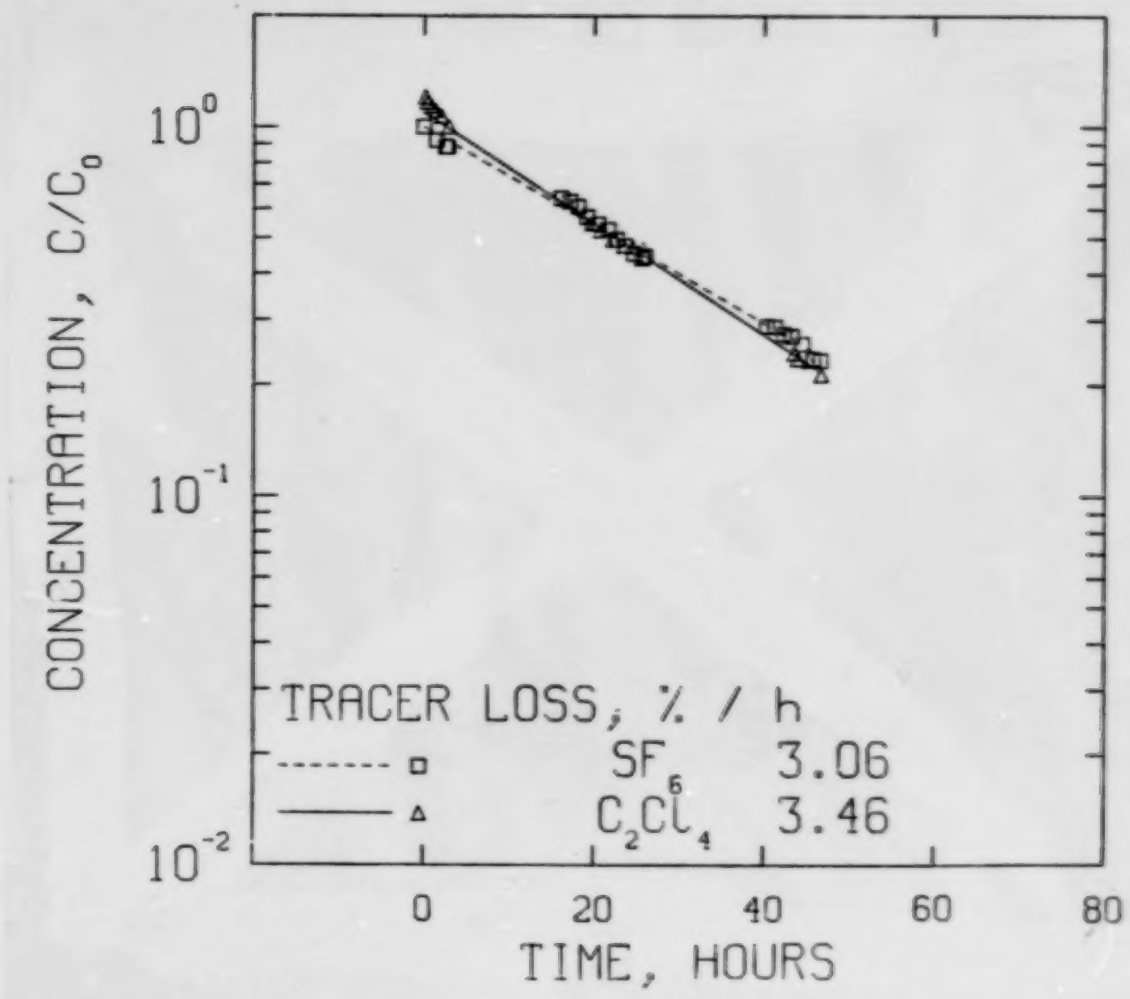

Figure C-7. Run 6-1: Perchloroethylene and SF_6 tracer gas concentration decreases for 6.0 m^2 of vinyl asbestos tile deposition surface.

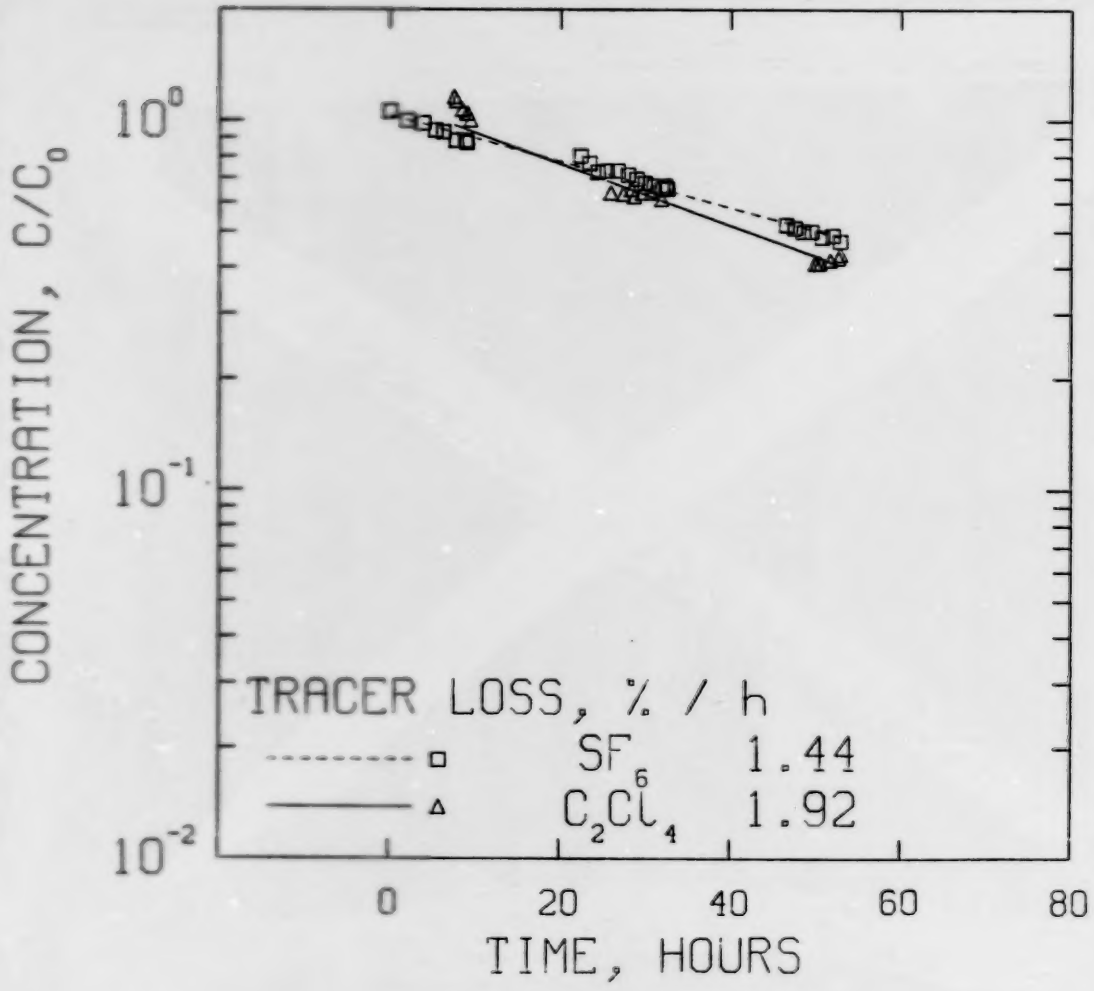

Figure C-8. Run 7-1: Perchloroethylene and SF_6 tracer gas concentration decreases for 6.0 m^2 of tar paper deposition surface.

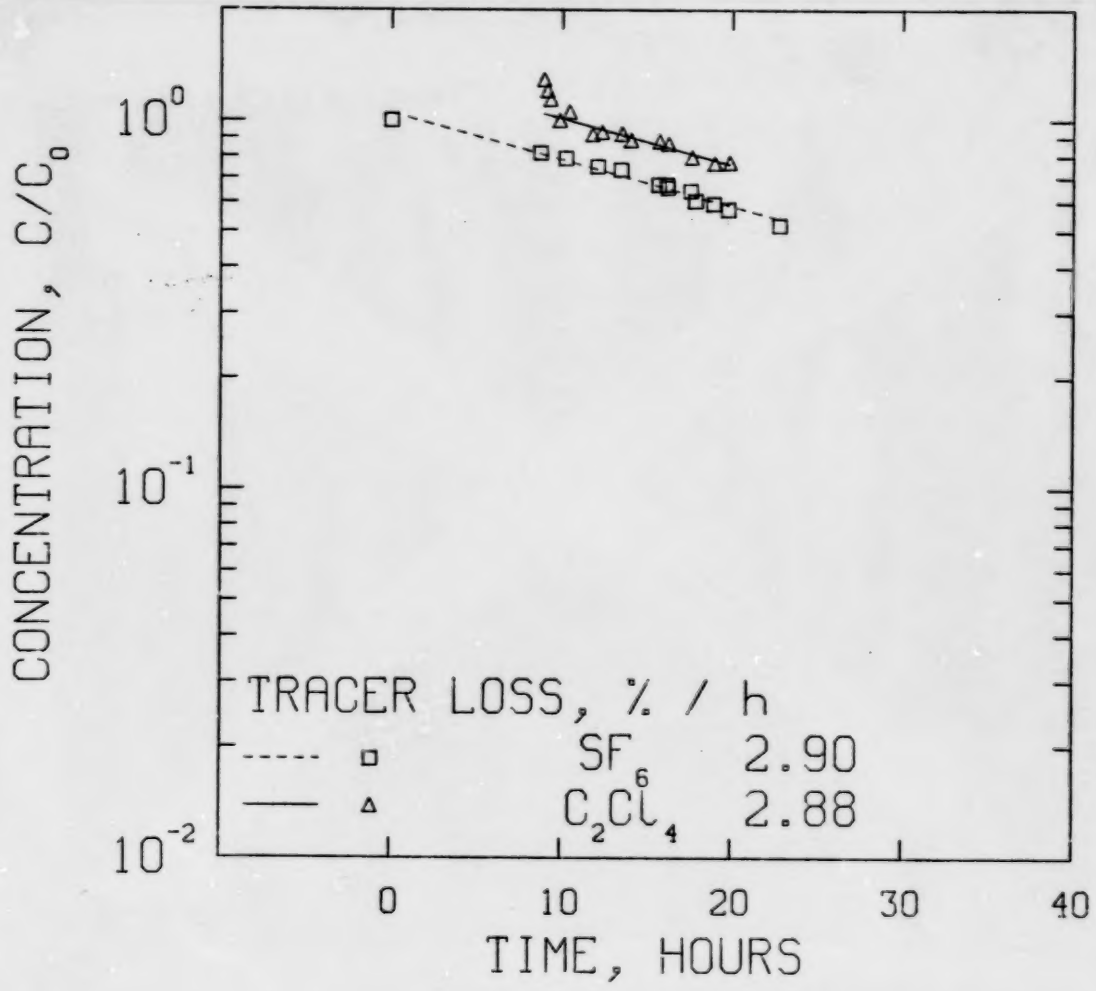

Figure C-9. Run 8-2: Perchloroethylene and SF_6 tracer gas concentration decreases for 6.0 m^2 of vinyl asbestos tile deposition surface.

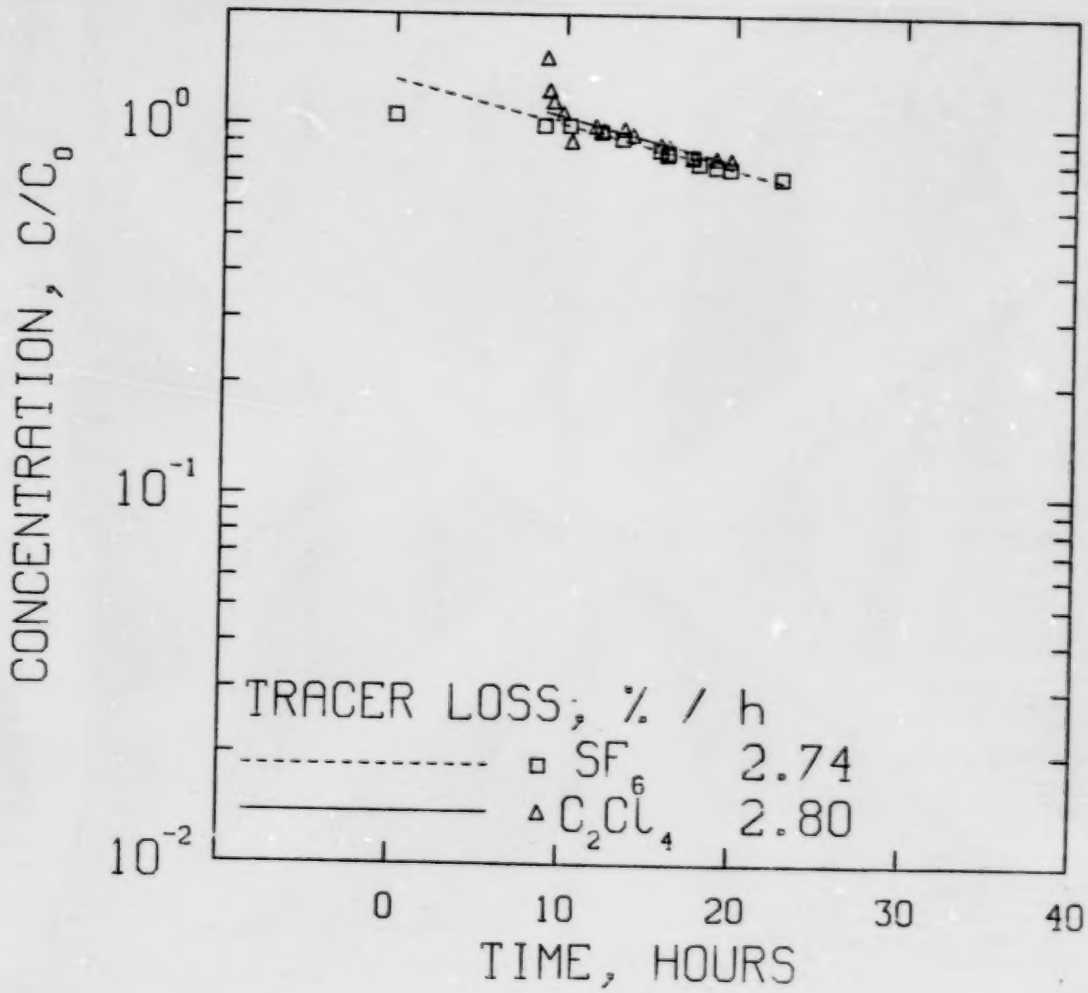

Figure C-10. Run 9-1: Perchloroethylene and SF_6 tracer gas concentration decreases for 6.0 m^2 of tar paper deposition surface.

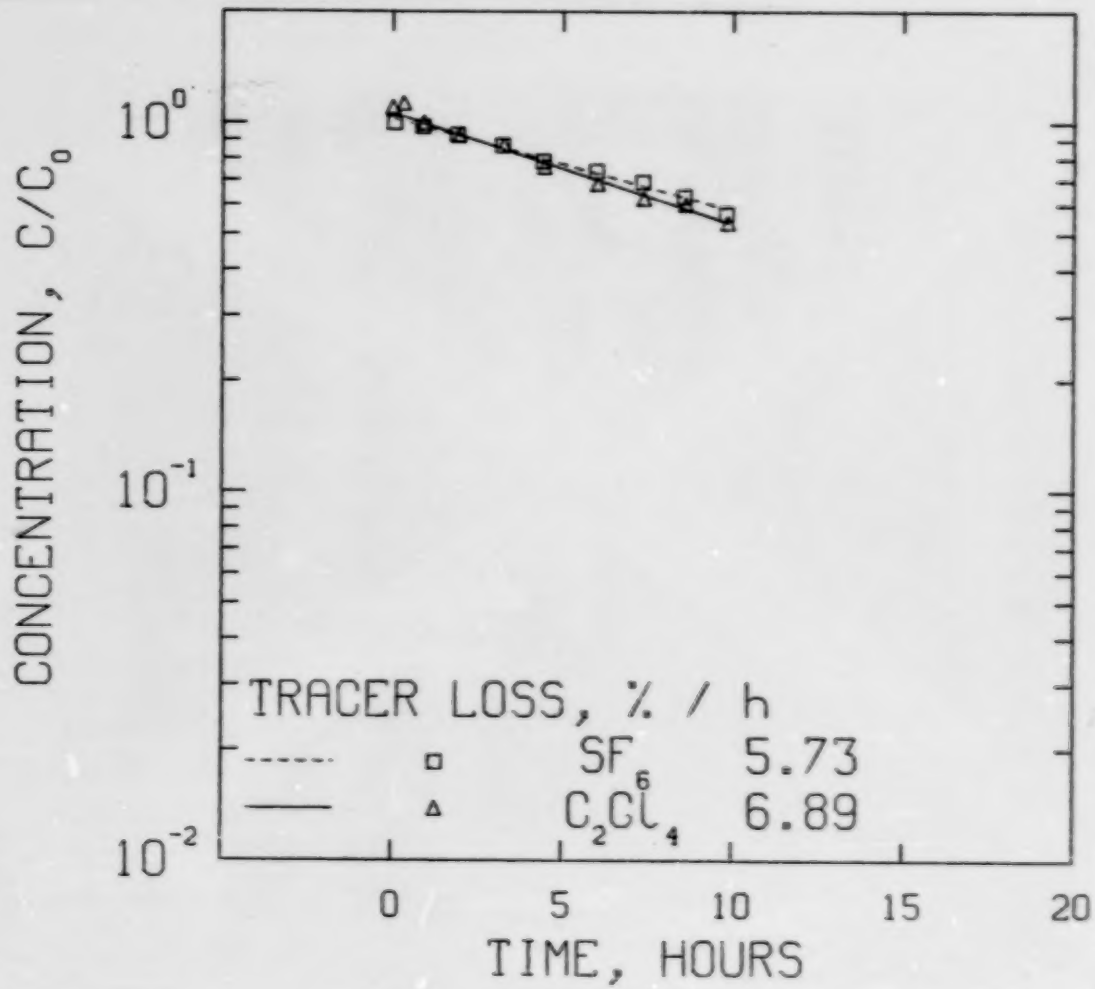

Figure C-11. Run 10-2: Perchloroethylene and SF_6 tracer gas concentration decreases for 6.0 m^2 of vinyl asbestos tile deposition surface.

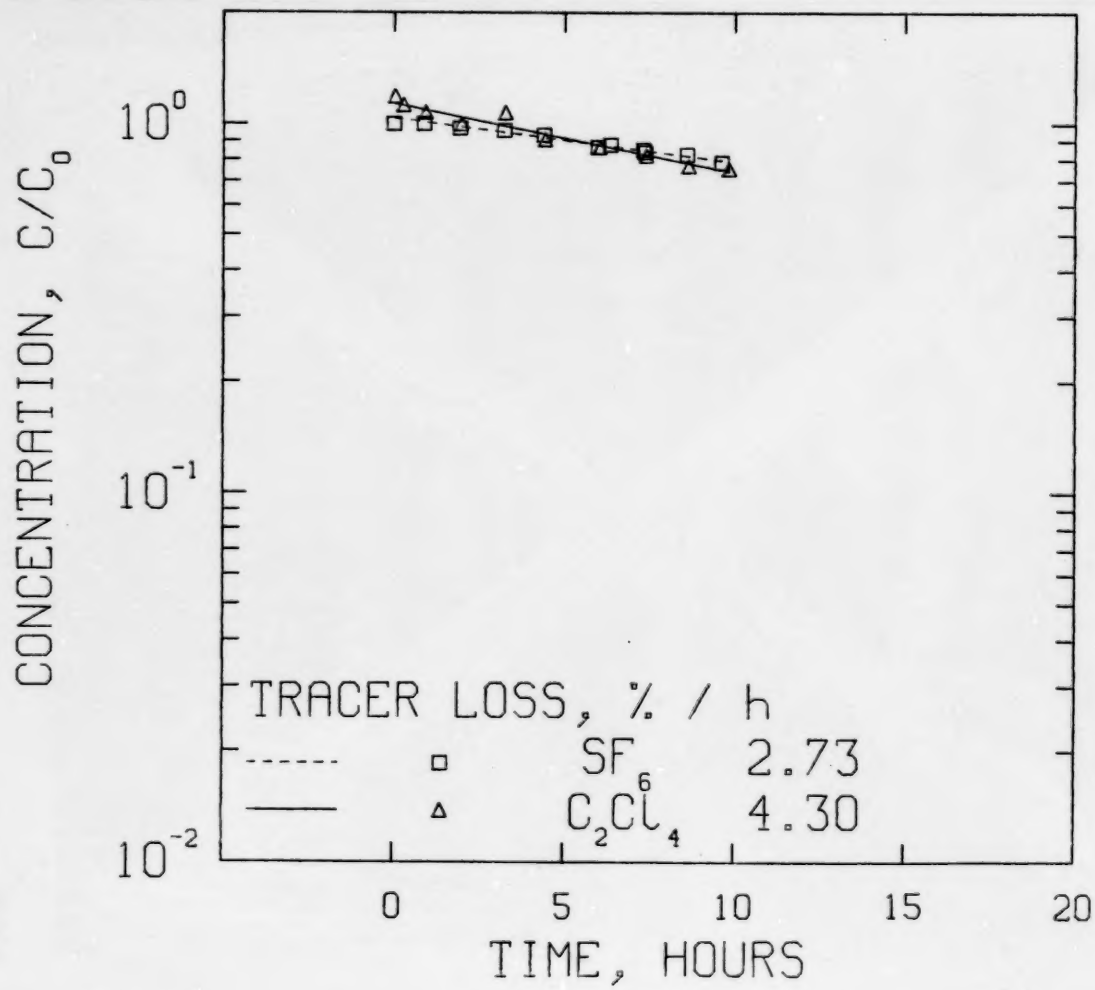

Figure C-12. Run 11-1: Perchloroethylene and SF_6 tracer gas concentration decreases for 6.0 m^2 of tar paper deposition surface.

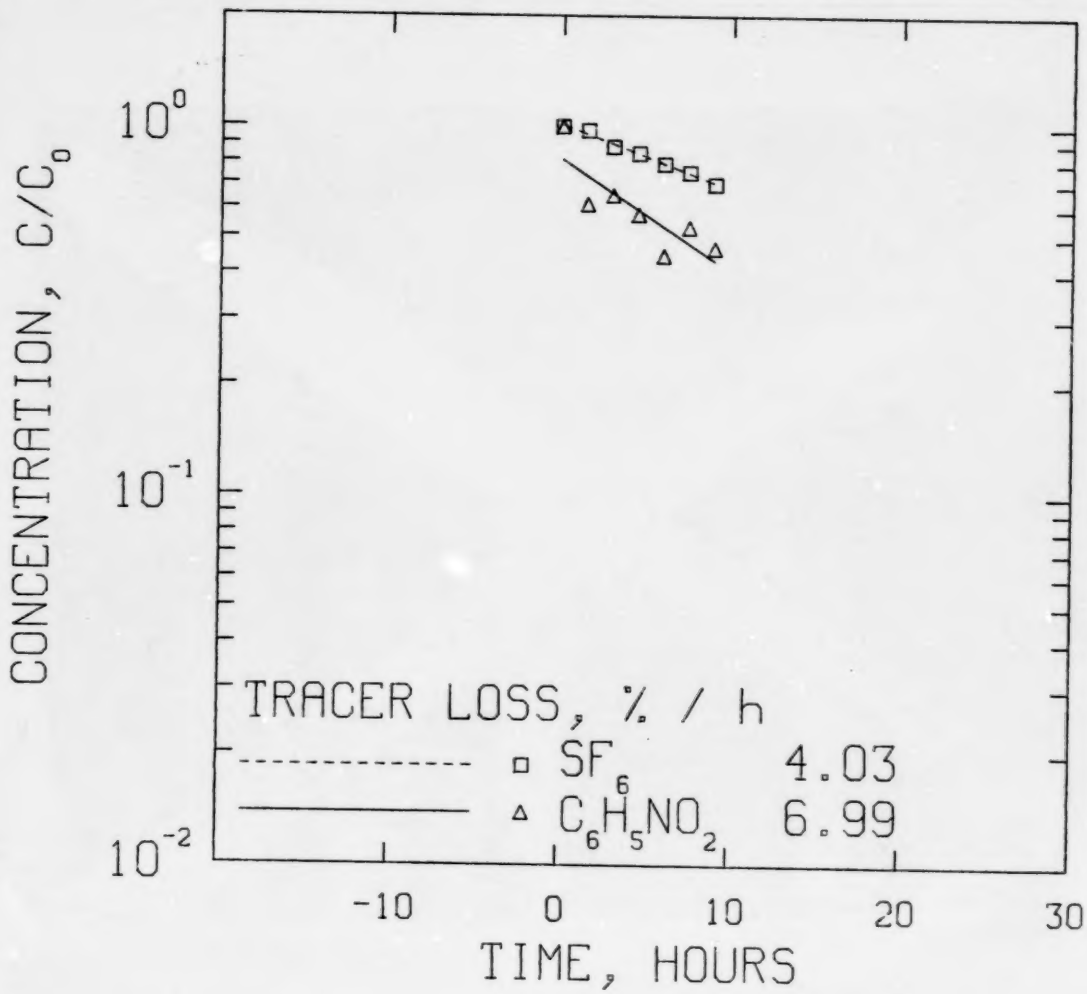

Figure C-13. Run 15-1: Nitrobenzene and SF_6 tracer gas concentration decreases for 6.0 m^2 of tar paper deposition surface.

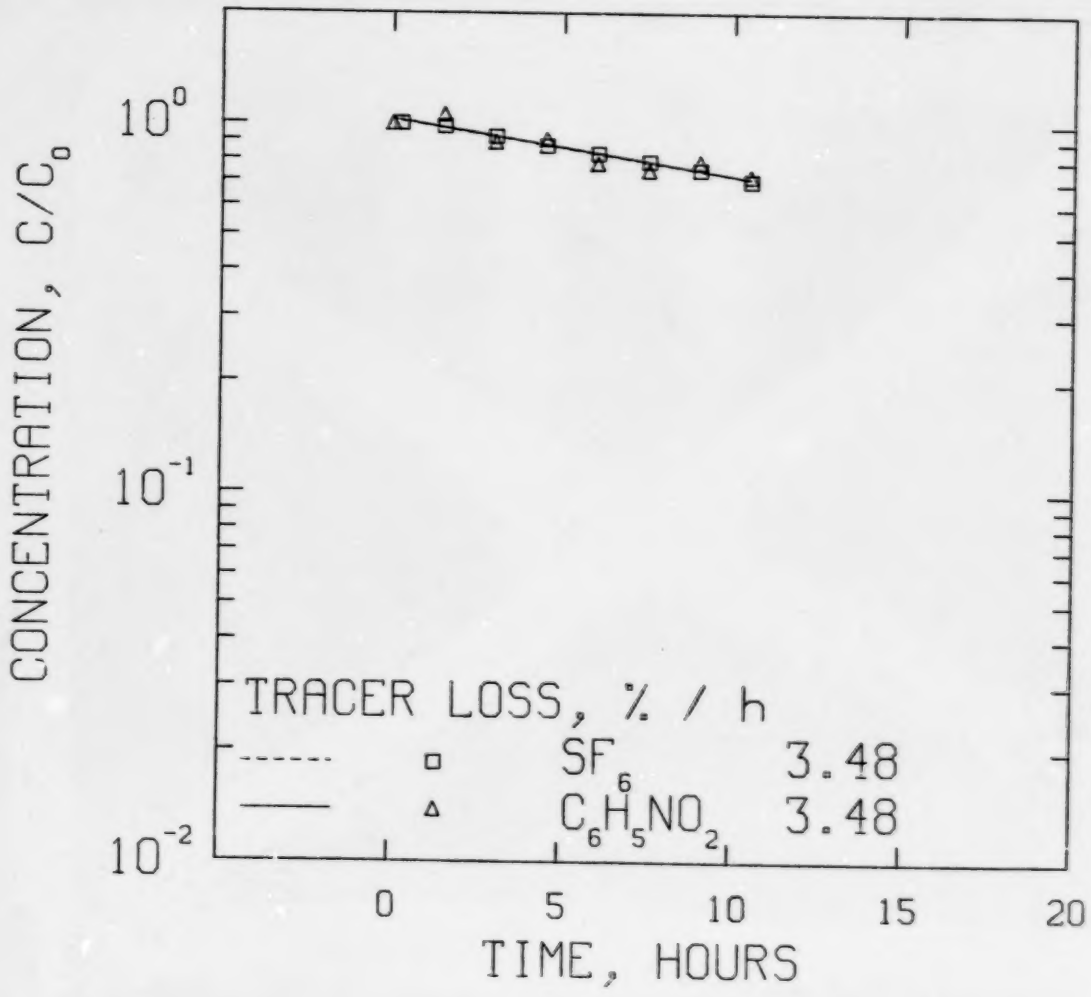

Figure C-14. Run 16-2: Nitrobenzene and SF_6 tracer gas concentration decreases for 6.0 m^2 of vinyl asbestos tile deposition surface.

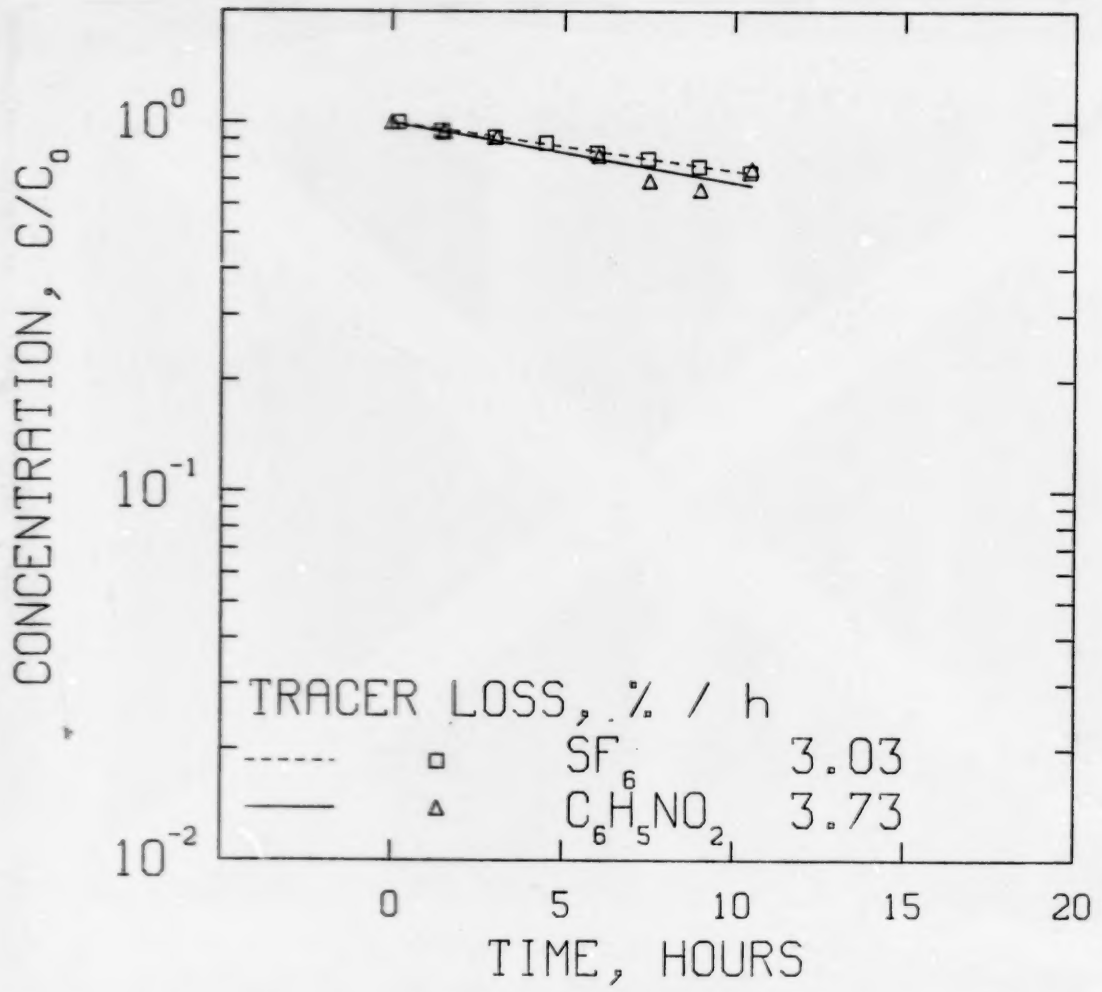

Figure C-15. Run 17-1: Nitrobenzene and SF_6 tracer gas concentration decreases for 6.0 m^2 of tar paper deposition surface.

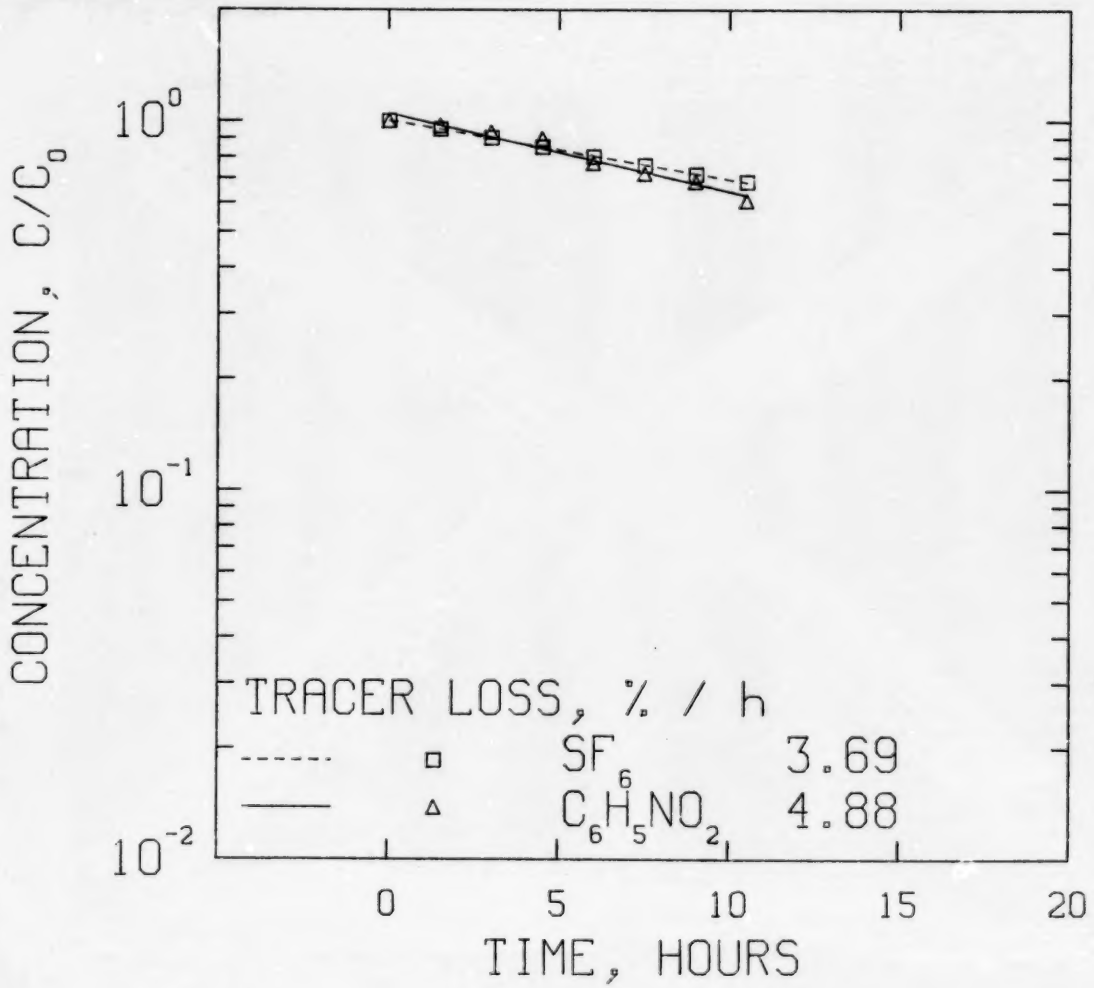

Figure C-16. Run 18-2: Nitrobenzene and SF_6 tracer gas concentration decreases for 6.0 m^2 of vinyl asbestos tile deposition surface.

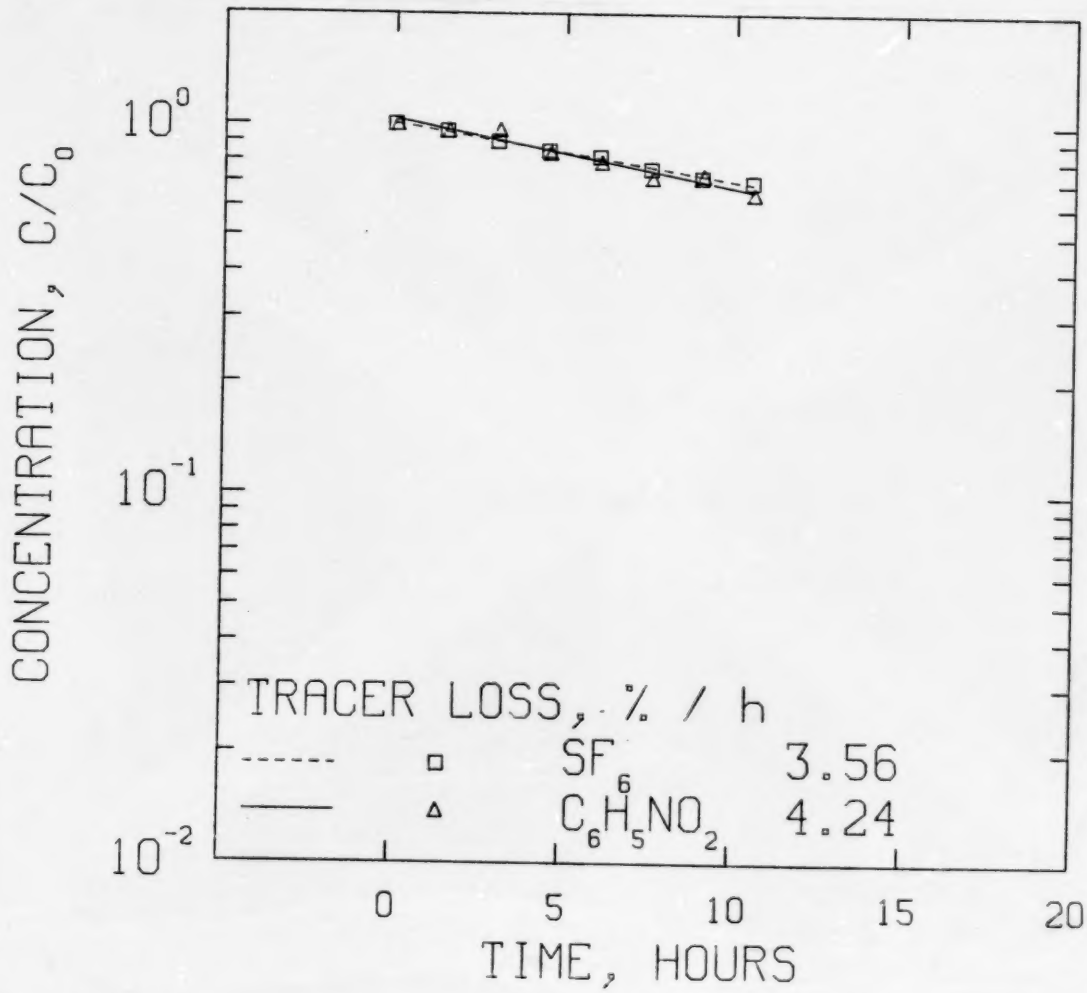

Figure C-17. Run 19-1: Nitrobenzene and SF_6 tracer gas concentration decreases for 6.0 m^2 of tar paper deposition surface.

APPENDIX D

HAP AND SF_6 CONCENTRATION DATA

Numerical values of hazardous air pollutant (HAP) and SF_6 concentrations obtained as a function of time in the two stirred chambers are listed in Tables D-1 through D-17. These data are shown as normalized concentrations in the figures of Appendix C. Concentrations were normalized by dividing each concentration by the concentrations noted by the asterisks in each table.

TABLE D-1. RUN 1-1: PERCHLOROETHYLENE AND SF_6 TRACER GAS CONCENTRATION DECREASES FOR 10.0 m^2 OF CEMENT BLOCK DEPOSITION SURFACE

HAP sampling data			SF_6 sampling data		
Day	Time (h.min)	Concentration (ppm)	Day	Time (h.min)	Concentration (ppm)
13	15.25	72.0*	13	11.00	2850*
13	15.31	80.2	13	12.00	2760
13	15.38	75.7	13	14.44	2540
13	15.43	73.6	14	20.33	871
13	16.02	72.5	14	20.36	905
14	21.01	16.9	16	05.19	292
14	21.08	15.9	16	05.22	387
14	21.13	16.7	16	05.25	378
14	21.19	18.6	16	05.28	327
14	21.27	18.3	16	05.40	421
16	06.02	6.3	16	05.44	404
16	06.08	7.7	16	22.07	215
16	06.15	6.3	16	22.10	206
16	06.23	7.2	17	14.28	129
17	01.17	4.4	17	14.33	129
17	01.25	4.0			
17	01.30	3.5			
17	17.13	2.1			
17	17.20	2.4			

*C_o for normalizing in figures.

TABLE D-2. RUN 1-2: PERCHLOROETHYLENE AND SF_6 TRACER GAS CONCENTRATION DECREASES FOR 6.1 m^2 OF CEMENT BLOCK DEPOSITION SURFACE

HAP sampling data			SF_6 sampling data		
Day	Time (h.min)	Concentration (ppm)	Day	Time (h.min)	Concentration (ppm)
13	16.09	138*	13	11.05	2600*
13	16.13	120	13	12.03	2560
13	16.20	129	13	14.50	2500
13	16.24	118	14	20.38	1090
13	16.28	111	14	20.41	1310
13	16.39	112	14	20.44	1320
14	21.32	49.7	16	05.32	714
14	21.38	54.2	16	05.36	722
14	21.43	38.7	16	22.14	447
14	21.48	51.1	16	22.17	464
14	21.56	43.0	16	22.20	464
16	07.07	28.6	17	14.36	335
16	07.18	26.7	17	14.39	344
16	07.24	25.4			
16	07.32	26.9			
17	00.50	23.1			
17	00.55	16.6			
17	01.06	21.6			
17	01.12	17.5			
17	01.36	16.2			
17	17.25	07.1			
17	17.32	11.2			
17	17.43	09.9			

*C_o for normalizing in figures.

TABLE D-3. RUN 2-1: PERCHLOROETHYLENE AND SF_6 TRACER GAS CONCENTRATION DECREASES FOR 10.0 m^2 OF CEMENT BLOCK DEPOSITION SURFACE

HAP sampling data			SF_6 sampling data		
Day	Time (h.min)	Concentration (ppm)	Day	Time (h.min)	Concentration (ppm)
25	10.07	44.7	25	12.13	2430*
25	11.11	64.3	25	13.12	2180
25	12.08	80.4*	25	14.14	2160
25	13.08	122	25	15.12	2230
25	14.08	106	26	10.13	1380
25	15.08	112	26	11.13	1340
26	09.08	52	26	12.11	1450
26	10.08	57.5	26	13.12	1360
26	11.07	58	26	14.13	1340
26	12.06	55.8	26	15.06	1210
26	13.06	54.3	27	14.52	584
26	14.08	47.7	27	15.51	620
26	15.01	53.1	28	11.09	258 **
27	14.45	26.9	28	12.04	293 **
27	15.47	27.1	28	13.05	301 **
			29	11.17	136 **
			29	12.15	124 **
			29	13.14	132 **
			31	14.30	54 **
			31	15.08	34 **

*C_o for normalizing in figures.

**Data points not used in calculating the SF_6 loss rate.

TABLE D-4. RUN 2-2: PERCHLOROETHYLENE AND SF_6 TRACER GAS CONCENTRATION DECREASES FOR 6.1 m^2 OF CEMENT BLOCK DEPOSITION SURFACE

HAP sampling data			SF_6 sampling data		
Day	Time (h.min)	Concentration (ppm)	Day	Time (h.min)	Concentration (ppm)
25	10.24	53.8	25	12.17	2570
25	11.24	67.1*	25	13.16	2670*
25	12.20	92.6	25	14.17	2710
25	13.19	88.7	25	15.15	2620
25	14.20	85.6	26	9.18	2030
25	15.20	82.4	26	10.17	2100
26	9.20	62.9	26	11.16	2140
26	10.20	59.8	26	12.14	2140
26	11.19	57.8	26	13.16	2100
26	12.19	56.3	26	14.17	2070
26	13.19	57.6	26	15.10	2000
26	14.20	53.8	27	14.55	1460
26	15.13	52	27	15.55	1500
27	14.58	33.1	28	11.12	1030 **
27	15.58	33.0	28	12.12	1020 **
			28	13.09	1020 **
			29	11.20	698 **
			29	12.18	670 **
			29	13.18	632 **
			31	14.34	271 **
			31	15.12	264 **

*C_o for normalizing in figures.

**Data points not used in calculating the SF_6 loss rate.

TABLE D-5. RUN 4-1: PERCHLOROETHYLENE AND SF_6 TRACER GAS CONCENTRATION DECREASES FOR 10.0 m^2 OF CEMENT BLOCK DEPOSITION SURFACE

HAP sampling data			SF_6 sampling data		
Day	Time (h.min)	Concentration (ppm)	Day	Time (h.min)	Concentration (ppm)
22	09.33	145*	22	09.53	1580*
22	10.22	130	22	11.48	1383
22	11.31	120	22	11.54	1361
22	12.43	104	22	13.15	1229
22	13.45	95.4	23	09.20	364
23	09.06	23.6	23	10.40	337
23	10.35	25.1	24	10.11	79.1
24	10.08	4.7	24	10.57	75.2
24	10.59	4.6	24	12.51	66.1
24	12.40	4.			

*C_o for normalizing in figures.

TABLE D-6. RUN 4-2: PERCHLOROETHYLENE AND SF_6 TRACER GAS CONCENTRATION DECREASES FOR 6.1 m^2 OF CEMENT BLOCK DEPOSITION SURFACE

HAP sampling data			SF_6 sampling data		
Day	Time (h.min)	Concentration (ppm)	Day	Time (h.min)	Concentration (ppm)
22	09.37	94.6*	22	10.05	2645*
22	10.25	89.4	22	11.50	2436
22	11.34	82.3	22	11.56	2480
22	12.46	75.5	22	13.22	2261
22	13.53	72.2	23	09.30	979
23	09.14	33.6	23	10.43	924
23	10.45	32.7	24	10.15	396
24	10.18	12.2	24	11.07	382
24	11.10	12.6	24	12.54	352
24	12.56	11.5			

*C_o for normalizing in figures.

TABLE D-7. RUN 6-1: PERCHLOROETHYLENE AND SF_6 TRACER GAS CONCENTRATION DECREASES FOR 6.0 m^2 OF VINYL ASBESTOS TILE DEPOSITION SURFACE

HAP sampling data			SF_6 sampling data		
Day	Time (h.min)	Concentration (ppm)	Day	Time (h.min)	Concentration (ppm)
1	13.39	161	1	13.31	791*
1	13.52	156	1	14.59	727
1	14.20	152	1	16.03	698
1	14.49	148	1	16.17	698
1	15.28	143*	2	5.38	507
1	16.23	134	2	6.41	497
2	9.15	73.5	2	7.38	482
2	10.14	70.2	2	8.42	452
2	11.40	66.4	2	9.59	432
2	12.00	66.1	2	11.12	417
2	13.00	63.8	2	12.12	392
2	14.00	63.4	2	13.10	377
2	15.12	62.6	2	14.12	358
3	9.03	32.6	2	15.09	348
3	9.30	31.5	2	15.32	353
3	10.47	31.2	3	5.50	228
3	12.15	28.5	3	6.49	227
			3	7.50	217
			3	8.47	214
			3	10.02	204
			3	11.18	186
			3	12.10	184

*C_o for normalizing in figures.

TABLE D-8. RUN 7-1: PERCHLOROETHYLENE AND SF_6 TRACER GAS CONCENTRATION DECREASES FOR 6.0 m^2 OF TAR PAPER DEPOSITION SURFACE

HAP sampling data			SF_6 sampling data		
Day	Time (h.min)	Concentration (ppm)	Day	Time (h.min)	Concentration (ppm)
1	14.40	236	1	7.13	885*
1	14.56	230	1	9.15	836
1	15.37	218	1	11.05	821
1	16.13	213*	1	12.30	786
1	16.37	204	1	13.27	777
2	9.05	130	1	14.55	737
2	10.33	129	1	16.00	737
2	11.30	133	1	16.11	727
2	11.50	127	2	5.34	670
2	12.47	130	2	6.36	641
2	13.47	130	2	7.33	606
2	15.04	125	2	8.38	611
3	9.10	83.6	2	9.54	611
3	9.40	83.6	2	11.07	596
3	10.55	85.2	2	12.07	581
3	11.54	86.4	2	13.05	566
3	12.06	88.3	2	14.08	556
			2	15.05	546
			2	15.29	556
			2	15.45	546
			3	5.45	436
			3	6.45	428
			3	7.45	418
			3	8.43	418
			3	9.58	403
			3	11.14	408
			3	12.06	393

*C_o for normalizing in figures.

TABLE D-9. RUN 8-2: PERCHLOROETHYLENE AND SF_6 TRACER GAS CONCENTRATION DECREASES FOR 6.0 m^2 OF VINYL ASBESTOS TILE DEPOSITION SURFACE

HAP sampling data			SF_6 sampling data		
Day	Time (h.min)	Concentration (ppm)	Day	Time (h.min)	Concentration (ppm)
8	23.03	138	8	14.08	852*
8	23.14	129	8	22.52	695
8	23.26	122*	9	00.21	672
8	23.59	107	9	2.13	639
9	00.33	113	9	3.35	627
9	1.54	98.1	9	5.47	571
9	2.27	99.6	9	6.17	571
9	3.37	98.5	9	6.20	560
9	4.09	94.6	9	7.41	549
9	5.50	94.0	9	7.58	516
9	6.22	92.6	9	9.02	507
9	7.45	85.2	9	9.54	489
9	9.05	82.1	9	12.54	443
9	9.58	82.4			

*C_o for normalizing in figures.

TABLE D-10. RUN 9-1: PERCHLOROETHYLENE AND SF_6 TRACER GAS CONCENTRATION DECREASES FOR 6.0 m^2 OF TAR PAPER DEPOSITION SURFACE

HAP sampling data			SF_6 sampling data		
Day	Time (h.min)	Concentration (ppm)	Day	Time (h.min)	Concentration (ppm)
8	22.56	185	8	14.05	952
8	23.06	151	8	22.50	896
8	23.20	141	9	00.19	896*
8	23.54	131	9	2.11	863
9	00.26	110*	9	3.26	829
9	1.50	121	9	5.39	773
9	2.17	118	9	6.04	751
9	3.31	119	9	6.07	762
9	4.02	115	9	7.33	740
9	5.41	108	9	7.55	711
9	6.10	107	9	8.56	697
9	7.36	101	9	9.46	688
9	8.56	99.5	9	12.49	652
9	9.48	98.4			

*C_o for normalizing in figures.

TABLE D-11. RUN 10-2: PERCHLOROETHYLENE AND SF_6 TRACER GAS CONCENTRATION DECREASES FOR 6.0 m^2 OF VINYL ASBESTOS TILE DEPOSITION SURFACE

HAP sampling data			SF_6 sampling data		
Day	Time (h.min)	Concentration (ppm)	Day	Time (h.min)	Concentration (ppm)
9	21.43	78.7	9	21.46	941*
9	22.02	80.6*	9	22.36	919
9	22.38	71.5	9	23.37	874
9	23.40	65.9	10	00.56	818
10	00.58	62.3	10	02.08	740
10	02.10	54.3	10	03.42	695
10	03.44	48.9	10	05.04	650
10	05.06	44.7	10	06.17	594
10	06.20	43.1	10	07.31	534
10	07.34	38.4			

*C_o for normalizing in figures.

TABLE D-12. RUN 11-1: PERCHLOROETHYLENE AND SF_6 TRACER GAS CONCENTRATION DECREASES FOR 6.0 m^2 OF TAR PAPER DEPOSITION SURFACE

HAP sampling data			SF_6 sampling data		
Day	Time (h.min)	Concentration (ppm)	Day	Time (h.min)	Concentration (ppm)
9	21.38	165	9	21.36	829
9	21.53	156	9	22.29	829*
9	22.32	149*	9	23.32	807
9	23.34	139	10	00.50	796
10	00.52	149	10	02.00	773
10	02.02	126	10	03.35	717
10	03.38	120	10	03.57	728
10	05.00	114	10	04.55	706
10	06.15	107	10	04.58	695
10	07.26	105	10	06.12	685
			10	07.13	652

*C_o for normalizing in figures.

TABLE D-13. RUN 15-1: NITROBENZENE AND SF_6 TRACER GAS CONCENTRATION DECREASES FOR 6.0 m^2 OF TAR PAPER DEPOSITION SURFACE

HAP sampling data		SF_6 sampling data	
Time (h.min)	Concentration ng/l	Time (h.min)	Concentration (ppm)
0.0	81.95*	0.0	978*
1.5	50.42	1.5	955
3.0	53.45	3.0	863
4.5	47.36	4.5	829
6.0	36.61	6.0	777
7.5	43.75	7.5	737
9.0	38.40	9.0	685

*C_o for normalizing in figures.

TABLE D-14. RUN 16-2: NITROBENZENE AND SF_6 TRACER GAS CONCENTRATION DECREASES FOR 6.0 m^2 OF VINYL ASBESTOS TILE DEPOSITION SURFACE

HAP sampling data			SF_6 sampling data		
Day	Time (h.min)	Concentration ng/l	Day	Time (h.min)	Concentration (ppm)
22	21.38	561*	22	21.53	1170*
22	23.08	593	22	23.09	1150
23	00.38	500	23	00.39	1080
23	02.08	509	23	02.09	1020
23	03.38	439	23	03.39	973
23	05.08	421	23	05.09	926
23	06.38	443	23	06.39	880
23	08.08	406	23	08.09	822

*C_o for normalizing in figures.

TABLE D-15. RUN 17-1: NITROBENZENE AND SF_6 TRACER GAS CONCENTRATION DECREASES FOR 6.0 m^2 OF TAR PAPER DEPOSITION SURFACE

HAP sampling data			SF_6 sampling data		
Day	Time (h.min)	Concentration ng/l	Day	Time (h.min)	Concentration (ppm)
22	21.38	186*	22	21.49	1900*
22	23.08	175	22	23.05	1800
23	00.38	170	23	00.35	1730
23	03.38	151	23	02.05	1670
23	05.08	129	23	03.35	1570
23	06.38	122	23	05.05	1510
23	08.08	139	23	06.35	1440
			23	08.05	1390

*C_o for normalizing in figures.

TABLE D-16. RUN 18-2: NITROBENZENE AND SF_6 TRACER GAS CONCENTRATION DECREASES FOR 6.0 m^2 OF VINYL ASBESTOS TILE DEPOSITION SURFACE

HAP sampling data			SF_6 sampling data		
Day	Time (h.min)	Concentration ng/l	Day	Time (h.min)	Concentration (ppm)
23	21.38	518*	23	21.39	1277*
23	23.08	503	23	23.09	1214
24	00.38	483	24	00.39	1150
24	02.08	464	24	02.09	1086
24	03.38	399	24	03.39	1022
24	05.08	373	24	05.09	969
24	06.38	355	24	06.39	915
24	08.08	315	24	08.09	873

*C_o for normalizing in figures.

TABLE D-17. RUN 19-1: NITROBENZENE AND SF_6 TRACER GAS CONCENTRATION DECREASES FOR 6.0 m^2 OF TAR PAPER DEPOSITION SURFACE

HAP sampling data			SF_6 sampling data		
Day	Time (h.min)	Concentration ng/l	Day	Time (h.min)	Concentration (ppm)
23	21.38	323*	23	21.34	1065*
23	23.08	311	23	23.05	1022
24	00.38	312	24	00.35	958
24	02.08	271	24	02.05	905
24	03.38	256	24	03.35	873
24	05.08	232	24	05.05	809
24	06.38	236	24	06.35	766
24	08.08	210	24	08.05	745

*C_o for normalizing in figures.